Plant Physiology and Biochemistry 216 (2024) 109117

Contents lists available at ScienceDirect

Plant Physiology and Biochemistry

journal homepage: www.elsevier.com/locate/plaphy

The Vacuolar H^+-ATPase subunit C is involved in oligogalacturonide (OG) internalization and OG-triggered immunity

Moira Giovannoni [a], Valentina Scafati [a], Renato Alberto Rodrigues Pousada [a], Manuel Benedetti [a], Giulia De Lorenzo [b], Benedetta Mattei [a,*]

[a] Department of Life, Health and Environmental Sciences, University of L'Aquila, 67100, L'Aquila, Italy
[b] Department of Biology and Biotechnology "C. Darwin", Sapienza University of Rome, 00185, Rome, Italy

ARTICLE INFO

Keywords:
Vacuolar H^+-ATPase
Oligogalacturonides
DAMPs
Endocytosis
Plant immunity

ABSTRACT

In plants, the perception of cell wall fragments initiates signal transduction cascades that activate the immune response. Previous research on early protein dynamics induced by oligogalacturonides (OGs), pectin fragments acting as damage-associated molecular patterns (DAMPs), revealed significant phosphorylation changes in several proteins. Among them, the subunit C of the vacuolar H^+-ATPase, known as DE-ETIOLATED 3 (DET3), was selected to elucidate its role in the OG-triggered immune response. The Arabidopsis *det3* knockdown mutant exhibited defects in H_2O_2 accumulation, mitogen-activated protein kinases (MAPKs) activation, and induction of defense marker genes in response to OG treatment. Interestingly, the *det3* mutant showed a higher basal resistance to the fungal pathogen *Botrytis cinerea* that, in turn, was completely reversed by the pre-treatment with OGs. Our results suggest a compromised ability of the det3 mutant to maintain a primed state over time, leading to a weaker defense response when the plant is later exposed to the fungal pathogen. Using fluorescently labelled OGs, we demonstrated that endocytosis of OGs was less efficient in the *det3* mutant, implicating DET3 in the internalization process of OGs. This impairment aligns with the observed defect in the priming response in the det3 mutant, underscoring that proper internalization and signaling of OGs are crucial for initiating and maintaining a primed state in plant defense responses.

1. Introduction

Plants have evolved sophisticated defense systems to safeguard themselves from attack launched by phytopathogenic organisms. Some of these defenses are constitutively present, such as physical and chemical barriers, e.g., plant cell wall. Others are activated only upon sensing a pathogen threat. The ability to swiftly detect danger and activate defense responses is vital for survival, constituting a fundamental aspect shared between plants and animals. Plant immunity is of the innate type and is triggered by the recognition of danger signals mediated by germ line-encoded recognition proteins. These proteins play a crucial role in sensing potential threats, initiating a cascade of defense responses aimed at neutralizing the invading pathogens and preserving plant health (Chisholm et al., 2006). Among the exogenous danger signals, pathogen-/microbe-associated molecular patterns (PAMPs/MAMPs) are conserved molecules secreted or constitutively present on the cell surface of a class of microbes. PAMPs, traditionally called elicitors, initiate the PAMP-triggered immunity (PTI), which effectively combats a broad spectrum of pathogens (Barrett and Heil, 2012). Additionally, plant immunity relies on the capacity to detect invading microbes through endogenous molecular patterns that emerge solely during tissue infection or damage, termed damage-associated molecular patterns (DAMPs). In these scenarios, the immune system is activated through the differentiation between intact self and altered self (De Lorenzo et al., 2001). Pattern recognition receptors (PRRs) play crucial roles in immunity, development, and reproductive processes by mediating the recognition of both endogenous and exogenous elicitors. These signaling molecules significantly influence the growth-defense trade-off (Pontiggia et al., 2020; Ngou et al., 2024).

PRRs encompass a broad range of cell membrane proteins formed by an ecto- and a trans-domain, usually devoted to pattern-recognition and interaction with other co-receptors, and an endo-domain, the latter devoted to the signal transduction (Boller and Felix, 2009). Among the various PRRs characterized to date are proteins with leucine rich repeats (LRRs) and lysine motifs (LysMs), G- and L-type lectins, Wall-associated kinases (WAKs) and Malectin/Malectin-like domain containing-proteins (Ngou et al., 2024).

* Corresponding author.
E-mail address: mariabenedetta.mattei@univaq.it (B. Mattei).

https://doi.org/10.1016/j.plaphy.2024.109117
Received 7 August 2024; Accepted 8 September 2024
Available online 13 September 2024

Abbreviations

AF	Alexa Fluor 488
AF-OGs	Alexa Fluor 488 labelled oligogalacturonides
BR	brassinosteroid
CYP81F2	cytochrome P450
DAMPs	damage-associated molecular patterns
DET3	DE-ETIOLATED 3
Elf18	elongation factor thermos unstable 18-amino acid long peptide
Flg22	flagellin 22-amino acid long peptide
FOX1	FAD-linked oxidoreductase 1
MAPK	mitogen-activated protein kinases
OGs	oligogalacturonides
PAD3	Phytoalexin deficient 3
PAMPs/MAMPs	pathogen-/microbe-associated molecular patterns
PGIP1	Polygalacturonase Inhibiting Protein 1
PRR	pattern recognition receptor
PTI	PAMP-triggered immunity
ROS	reactive oxygen species
TGN/EE	Trans-Golgi Network/early endosome compartment
UBQ5	ubiquitin 5
Vacuolar H + -ATPase	V-ATPase

Oligogalacturonides (OGs) are oligomers of α-1,4-linked galacturonosyl residues that act in plants as typical DAMPs (De Lorenzo et al., 2011). OGs trigger a broad range of defense responses, including the accumulation of secondary metabolites with antimicrobial activity (Cervone et al., 1989; Hahn, 1981; Tsuji et al., 1992), ROS production [mediated, in *Arabidopsis thaliana*, by the RESPIRATORY BURST OXIDASE HOMOLOG D (RbohD)] and the reinforcement of cell wall by the *in muro* synthesis of callose (Galletti et al., 2008). Perception of molecular signals at the cell membrane by PRRs induces a signal transduction cascade that activates plant defenses; nevertheless, many of the mechanisms through which the OG signal is transduced remain unclear. Early responses triggered by OGs and the bacterial PAMP flg22, a 22-amino acid peptide localized in the domain 1 (D1) of bacterial flagellin, coincide in large part (Denoux et al., 2008).

For example, mitogen-activated protein kinases (MAPKs) are activated within minutes upon perception of both OGs and flg22 (Bethke et al., 2012; Boudsocq et al., 2010; Rasmussen et al., 2012). The response to OGs and flg22 is mainly mediated by the MAP kinases MPK3 and MPK6 (Asai et al., 2002; Galletti et al., 2011).

In a previous study, various protein clusters of *A. thaliana* with a potential involvement in molecular signaling were identified as phospho-regulated in response to OGs (Mattei et al., 2016). Among these clusters, the ATP synthase cluster encompassed different subunits of the Vacuolar type H^+-ATPase (V-ATPase; A, C and E1 subunits), all of which are similarly regulated by dephosphorylation in response to OGs (Mattei et al., 2016). V-ATPase is localized in the vacuolar (tonoplast) and Trans-Golgi Network (TGN) membranes, where it plays an important in the endocytic/secretory traffic (Luo et al., 2015; Schumacher and Krebs, 2010) and Ca^{2+} signaling (Allen et al., 2000; Peiter, 2011; Tang et al., 2012). DET3, the subunit C of the V-ATPase, was identified in detergent-resistant membranes of flg22-treated Arabidopsis suspension cells through quantitative mass spectrometric analysis (Keinath et al., 2010), suggesting a change in membrane compartmentalization during elicitation and a potential role in elicitor-induced immune responses, possibly through alterations in membrane dynamics.

The characterization of the *det3* mutant, initially isolated for its photomorphogenic phenotype in the dark (Cabrera y Poch et al., 1993; Schumacher et al., 1999), revealed complex defects, including a conditionally reduced hypocotyl cell expansion due to ethylene- and jasmonate-mediated growth inhibition, ectopic lignification, increased starch levels, altered meristem activity in response to brassinosteroid (BR) and a reduced stomatal closure in response to extracellular Ca^{2+} but not to ABA (Schumacher and Krebs, 2010; Szekeres et al., 1996). The *det3* mutant carries a point mutation (t1592a) in the first intron of *DET3* gene that impairs the RNA splicing at the 3' site due to destruction of a branchpoint consensus sequence, thereby leading to approximately a 50% reduction of both mRNA and DET3 protein levels as well as a diminished V-ATPase activity. The mutant shows an aberrant plant phenotype (Fukao and Ferjani, 2011; Schumacher et al., 1999), highlighting the importance of V-ATPase complex in the regulation of Arabidopsis growth and morphogenesis. The reduced V-ATPase activity was also associated to an increased pH of the TGN/early endosome (TGN/EE) compartment and alterations of the transport and recycling of important vital components of the cell membrane, such as the BR receptor and cellulose synthase complex (Luo et al., 2015). This negative impact could account for the characteristic BR insensitivity and altered cellulose content observed in the *det3* mutant (Luo et al., 2015).

Moreover, despite normal levels of the flg22 receptor FLS2, the *det3* mutant responded to flg22 with increased MAPK activation and stomata closure, and was more susceptible to bacterial infection, suggesting an important role of V-ATPase in PAMP-triggered immunity (Keinath et al., 2010). These insights indicate a crucial role of DET3 in the physiology of the plant and explain the lethality associated with the total loss of its function (Schumacher et al., 1999). In this work, the involvement of *DET3* in DAMP-triggered immunity was investigated using OGs as representative cell wall DAMP.

2. Materials and methods

2.1. Elicitors and plant material

The elicitors used in this study are a mixture of unsubstituted OGs with a degree of polymerization ranging from 10 to 15, hereafter referred to as OGs, purchased from Biosynth Carbosynth (https://www.biosynth.com/p/OG59704/galacturonan-dp10-dp15-sodium-salt) and a flg22 oligopeptide purchased from EZBiolab (http://store.ezbiolab.com/cp7201.html). The plants used in this study are *Arabidopsis thaliana* ecotype Columbia-0 (Col-0). The *det3* mutant (Col-0 genetic background) derived from a diepoxy butane-mutagenized population has been previously described (Cabrera y Poch et al., 1993) and was provided by Prof. Ralph Panstruga (Institute for Biology I of RWTH Aachen University, Germany).

2.2. Plant growth conditions

Arabidopsis plants were grown in a chamber "Phytotron SGC2" (Weiss Technik) at 22 °C and 60% relative humidity under 16/8 h light/dark cycle (~120 μmol $m^{-2}.sec^{-1}$). For adult plant assays, seeds were directly germinated on soil (Compo Sana). For seedling assays, seeds were firstly surface sterilized [0.01% w/v sodium dodecyl sulfate (SDS), 1.6% v/v NaClO] for 10 min and then were washed with sterilized water. Washed seeds were germinated and grown (10/well) in 2 mL of 0.5X Murashige and Skoog (MS) medium pH 5.7 supplemented with 0.5% sucrose in multi-well plates.

2.3. Measurement of the alkalinization of the growth medium

For the measurement of the alkalinization of the growth medium, washed seeds (Col-0 and *det3* mutant), prepared as described in paragraph 2.2, were germinated in flasks containing 20 mL of 0.5X MS medium supplemented with 0.5% (w/v) sucrose. 10 days-old seedlings were treated with OGs (100 μg mL^{-1}), flg22 (10 μM) or water as control. A pH-meter (pH Meter Basic 20, Crisom) was used to measure the pH changes in the culture medium at 10-s intervals after treatment with

elicitors for 5 min (shorter times) and at 30-min intervals for 3 h after treatments (longer times).

2.4. Oxidative burst assay

The accumulation of H_2O_2 produced during incubation with elicitors was determined using the spectrophotometry-based ferrous oxidation-xylenol orange method (Jiang et al., 1990; Scortica et al., 2022, 2023) with some modifications. We chose the xylenol orange assay for measuring the oxidative burst because, unlike the luminol-HRP coupled assay, it is not affected by pH changes (Bolwell et al., 2002). H_2O_2 released in the culture medium was measured by using the xylenol orange assay (Scortica et al., 2023). Ten-day-old seedlings of wild type and *det3* plants were treated with OGs (50 μg mL^{-1}), flg22 (10 nM) and water. An aliquot (100 μL) from each elicitor-supplemented growth medium was combined with 100 μL of the assay reagent (0.5 mM ammonium iron(ii) sulfate, 50 mM H_2SO_4, 0.2 mM xylenol orange and 200 mM sorbitol). Absorbance at 560 nm was measured at 0 (without treatments), 10, 30, 60, 90, 180 min after treatment with elicitors. Data were expressed as pmol $H_2O_2.mg^{-1}$ FW seedlings * mL.

2.5. Protein extraction and MAPK immunoblotting

For the immunoblotting assays, seedlings were grown under the controlled conditions previously olutlined.

9 day-after growth, the culture medium was adjusted to 1 mL, and 24 h later, Arabidopsis seedlings were treated with OGs (50 μg mL^{-1}) and flg22 (10 nM) for 10 and 30 min. The phosphatase-inhibiting buffer [50 mM Tris–HCl pH 7.5, 200 mM NaCl, 1 mM EDTA, 20 mM NaF, 2 mM Na_3VO_4, 1 mM Na_2MoO_4, 10% (v/v) glycerol, 0.1% (v/v) Tween-20, 1 mM DTT, 1 mM phenyl-methyl-sulfonyl fluoride, phosphatase inhibitor cocktail P9599 (Sigma-Aldrich)] was used to extract the total proteins from Arabidopsis seedlings (n = 20, about 100 mg DW). The bradford reagent (Bio-Rad) was used to quantify the protein content in the plant extracts. For each sample, total protein extract (40 μg) was separated by SDS- PAGE 8% and analyzed by Western blot analysis. The equal loading of samples was determined by staining the membrane with Ponceau-S Red. The immunodetection of phosphorylated MAPKs was performed with an α-p44/42-ERK antibody (1:2000 dilution, Cell Signaling Technology). Thereafter, an α-AtMPK3 (1:2500 dilution, Sigma, M8318) and α-AtMPK6 (1:10000 dilution, Sigma, A7104) antibodies were used to detect the MPK3 and MPK6 proteins, respectively. Membranes were then incubated in Tris-buffered saline, 0.1% Tween 20 (TBS-T) containing 0.5% (w/v) BSA (bovine serum albumin) with a secondary horseradish peroxidase-conjugated anti-rabbit antibody (1:6000 dilution, Bio-Rad). The Clarity™ Western ECL substrate detection kit (Bio-Rad) and the Alliance Q9 imaging system (UVITEC Cambridge) were used for digital imaging.

2.6. Gene expression analysis

For gene expression analysis, seedlings were grown under controlled conditions as described above. After 9 days of growth, the volume of culture medium was adjusted to 1 mL, and 24 h later, Arabidopsis seedlings were treated with OGs (50 μg mL^{-1}) and flg22 (10 nM), for 1 and 3 h. Plant tissues were pulverized by using MM301 Ball Mill (Retsch, Basel, Switzerland) for 1 min at 24 Hz. Total RNA extraction, cDNA synthesis and quantitative real-time polymerase chain reaction (qRT-PCR) were performed in accordance with Giovannoni et al., 2021a. Gene expression levels were normalized against the reference gene *UBIQUITIN 5* (*UBQ5*, At4G05320) and the data were analyzed with LinRegPCR software in accordance with Ruijter et al. (2013). The gene expression analysis was performed on three different biological replicates (each of them composed of three technical replicates) and the results obtained were averaged. The primers used for the qRT-PCR analysis are listed in Supplementary Table S1.

2.7. Botrytis cinerea infection assay

The fungus *Botrytis cinerea* was grown for 20 days at 22 °C on MEP medium [malt-agar 2% (w/v), peptone 1% (w/v) and micro-agar 1.5% (w/v)] until sporulation and then, it was maintained at 20 °C in a dark chamber in accordance with Giovannoni et al., 2021c. Subsequently, the infection assays were performed in accordance with (Ferrari et al., 2007; Giovannoni et al., 2021b; Giovannoni et al., 2021c). For elicitor-induced protection, plants were treated by spraying with water, OGs (200 μg mL^{-1}) or flg22 (1 μM) 24 h before fungal inoculation. *B. cinerea* infection was assessed 48 h after inoculation by measuring the lesion areas (mm^2) of infected leaves. 48 h post infection, a disease-resistance (DR) rating was assessed using a rating scale as previously described (Fabian et al., 2023; Wang et al., 2011) with some modifications. In brief, DR values ranging from 1 to 5, were scored as follows: value 1 = no or small lesion, rare symptoms; value 2 = lesions on 10%–30% of leaf surface; value 3 = lesions on 30%–50% of leaf surface; value 4 = lesions on 50%–70% of leaf surface, profuse necrosis; value 5 = lesions on over 70% of leaf surface, decayed/dead symptoms. Then, the lesion areas and DR values were measured by using the ImageJ software (https://imagej.nih.gov/ij).

2.8. Oligogalacturonide labelling with Alexa Fluor 488 (AF-OGs)

The OGs were conjugated to aminooxy derivative of the Alexa Fluor dye 488 (A30629, Invitrogen, http://www.invitrogen.com/) as previously described (Mravec et al., 2014) with minor modifications. In brief, OGs were incubated with Alexa Fluor 488 in water at a ratio of 0.5 equivalent moles. The reaction mixture was firstly incubated at 37 °C in dark condition for 24 h under gentle shaking (900 rpm) and then was incubated at room temperature for additional 24 h. The reaction mixtures were stored at −20 °C and used for downstream applications without any additional purification. The ability of AF-OGs to induce the expression of the defense marker gene *FOX1* was evaluated in 10-day--old wild type seedlings according to the conditions described in paragraph 2.2.

2.9. Confocal laser scanning microscopy using AF-OGs and FM4-64 labelling

Seven-day-old wild type and *det3* seedlings were treated for 30 min with AF-OGs (50 μg mL^{-1}) and AF, the latter used as a control. Labelled root samples with AF-OGs were scanned using a Leica SP5 TCS SP5 II confocal system (488 nm of excitation and 500–540 nm of emission) with 63X oil immersion lens.

The staining with FM™4–64 dye (2 μM, Invitrogen ™, T13320) was performed according to Giovannoni et al., 2021c. Labelled root samples with FM4-64 were scanned using a Leica SP5 TCS SP5 II confocal system (516 nm of excitation and 640 nm of emission) with 63X oil immersion lens. Z-stack images were collected over a length of 1.5 μm with 0.4 μm intervals to acquire signals. The images were processed by using the ImageJ software (https://imagej.nih.gov/ij) for contrast and brightness enhancement and they were treated equally (Tang et al., 2012).

3. Results

3.1. Elicitor-induced extracellular alkalinization and extracellular H_2O_2 accumulation are higher in det3 mutant seedlings

The altered phenotype of the *det3* mutant, carrying a single mutation (t1592a) localized in the first intron of *DET3* gene (Supplementary Data S1, Supplementary Fig. S1a) was assessed. The plants exhibited a stunted growth at each developmental stage, resulting in a dwarf phenotype and reduced biomass production compared to wild-type (Col-0) plants (Supplementary Fig. S1b), in agreement with previous observations (Schumacher et al., 1999). Next, we investigated whether, besides being

altered in the pH (increased) of the TGN/EE (Luo et al., 2015), the *det3* mutant also shows an alteration of apoplastic pH. The natural pH of extracellular environment is typically acidic in healthy plants and can dynamically change in response to various environmental stimuli and physiological factors (Boller and Felix, 2009; Geilfus, 2017). Indeed, extracellular alkalinization represents one of the earliest and most simply measurable response in the context of PTI (Boller and Felix, 2009; Geilfus, 2017; Huffaker et al., 2006). We observed that under resting conditions, the extracellular pH of *det3* mutant seedlings grown in liquid medium was slightly higher (6.2 ± 0.05) than that of Col-0 wild-type seedlings (5.85 ± 0.05), pointing to a tendency of *det3* mutants to alkalize the extracellular environment (Fig. 1a and b; *see* solid- and dashed-lines with black circles, i.e., H_2O-treatment). pH variations of the culture medium were also measured over time in response to OG and flg22. The *det3* mutant seedlings were able to further alkalinize the extracellular environment in response to OGs and flg22 (Fig. 1a and b; *see* solid- and dashed-lines with grey/white circles), although the maximal net increase of pH, as observed after 12 min from the treatment with the elicitors, was lower (+0.16) than that of wild type seedlings (+0.28), however reaching a pH even slightly higher than that of the elicited wild type (Fig. 1b). These results indicate that the DET3 subunit is relevant also for the apoplastic pH homeostasis, thereby suggesting that V-ATPases and cell membrane H^+-ATPases work together to regulate the pH of plant tissues both in rest conditions and in response to elicitors (Boller and Felix, 2009; Elmore and Coaker, 2011; Jeworutzki et al., 2010).

We then investigated a typical early apoplastic immune response induced by OGs and flg22, i.e. the accumulation of H_2O_2. This was measured in the culture medium of seedlings treated with OGs and in parallel with flg22, using the xylenol orange assay. In the elicitor-treated seedlings, the accumulation of H_2O_2 was significantly higher (6–8X) in the culture medium of *det3* mutant than in that of wild type (Fig. 1c and d, Supplementary Fig. S1).

3.2. OG-induced MAPK phosphorylation and defense marker gene expression are decreased in det3 mutant seedlings

Next, we examined the role of *DET3* in other response to OGs and

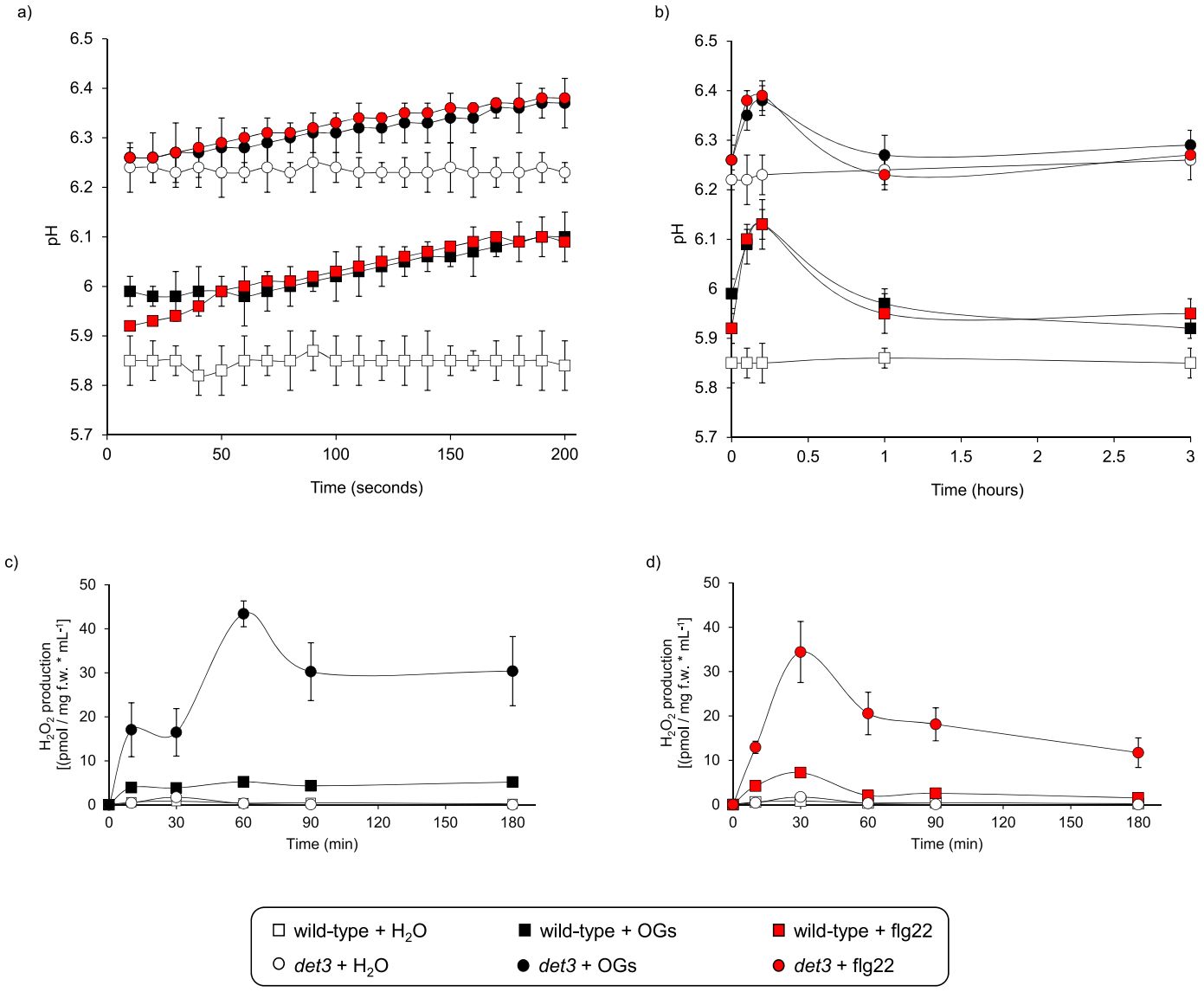

Fig. 1. Analysis of extracellular alkalinization and H_2O_2 production in elicitor-treated wild-type and *det3* seedlings. a, b) Extracellular alkalinization in wild-type and *det3* seedlings at a) short and b) longer times after treatments with OGs and flg22. Bars represent mean ± SD (n = 5). c, d) H_2O_2 accumulation in the growth medium of wild-type and *det3* seedlings after treatments with (c) OGs or (d) flg22 for the indicated time. Bars represent mean ± SD (n = 3). In all the experiments here reported, the treatment with water (H_2O) was used as negative control.

flg22. The phosphorylation status of MPK3 and MPK6 in elicitor-treated *det3* mutant seedlings was examined, since DET3 was found to be phospho-regulated after elicitation with OGs (Mattei et al., 2016). The immuno-decoration analysis was performed using the anti-pTpY antibody (Ichimura et al., 2002; Zhang and Dong, 2007). Compared to wild type plants, the phosphorylation of MPK6 and MPK3 in the *det3* mutants showed a slight decrease at 10 min with both elicitors whereas it was clearly decreased after 30 min after OG treatment only (Fig. 2a). After 30 min, phosphorylation was markedly higher in the *det3* mutant after flg22 treatment (Fig. 2a), in accordance with previous observations (Keinath et al., 2010). No differences in the basal phosphorylation status (water treatment) were observed. These results indicate that a reduced level of DET3 alter the OG- and flagellin-triggered phosphorylation of MAPKs in an opposite manner.

To further investigate whether *det3* mutants exhibit alterations in response to elicitor treatments, the expression level of four defense-related genes known to be induced by OGs was analyzed by qRT-PCR, namely *FOX1* (At1g26380) and *CYP81F2* (AT5G57220), which generally peak at around 1 h after elicitation (early induced genes), and *PAD3* (AT3G26830) and *PGIP1* (AT5G06860), which generally reach their highest expression 3 h after elicitation (late induced genes) (Denoux et al., 2008; Galletti et al., 2008; Gravino et al., 2017). *FOX1* encodes a flavoenzyme belonging to the berberine bridge enzyme-like (BBE-l) protein family, a class of FAD-dependent enzymes that act as defense proteins in *A. thaliana* (Benedetti et al., 2018; Locci et al., 2019; Pontiggia et al., 2020). In particular, FOX1 converts indole-cyanohydrin into indole-3-carbonyl nitrile, a secondary metabolite with antimicrobial activity (Boudsocq et al., 2010; Rajniak et al., 2015). *CYP81F2* encodes a cytochrome P450 monooxygenase involved in the biosynthesis of indole glucosinolate, a secondary metabolite produced in response to elicitor treatment (Asai et al., 2002; Nafisi et al., 2007). *PAD3* is involved in the biosynthesis of phytoalexins and plays a major role in providing resistance against the necrotrophic fungus *Botrytis cinerea*, whereas *PGIP1* encodes an extracellular leucin-rich repeat (LRR) protein that acts as inhibitor of several fungal polygalacturonases (Ferrari et al., 2003). Compared to wild-type plants, the *det3* mutant showed a reduced expression of *FOX1* and *PAD3* only in response to OG treatment, and of *CYP81F2* and *PGIP1* in response to both OG and flg22 treatments (Fig. 2b); levels of transcript of *FOX1* and *PAD3* were similar to the wild-type in response to flg22. Basal levels of all gene were higher in the mutant, except for *PGIP1* (Fig. 2b).

In summary, in the *det3* mutant, both the phosphorylation status of MPK3 and MPK6 and the induction of defense marker genes were markedly decreased in response to OGs, whereas the same defense responses were only partially affected in response to flg22 (Fig. 2).

3.3. Basal and elicitor-induced resistance against Botrytis cinerea is altered in det3 mutant plants

To further investigate the involvement of *DET3* in immunity, the basal and elicitor-induced resistance against the necrotrophic fungus *B. cinerea* was investigated. Both the leaf lesions caused by the fungus and the macroscopic disease symptoms, the latter assessed using specific DR values, were evaluated (Fig. 3). Compared to wild type plants, the *det3* mutant plants exhibited a significantly enhanced resistance against *B. cinerea* infection, since lesion areas and disease symptoms were both reduced in pathogen-inoculated leaves (Fig. 3a–c). Protection against *B. cinerea* can be promoted in Arabidopsis plants by pre-treating them with OGs or flg22 (Ferrari et al., 2007; Giovannoni et al., 2021b; Giovannoni et al., 2021c). The consequence of such pre-treatment is the acquisition of a 'primed' state that make plants more responsive to subsequent stimuli of both biotic and abiotic origin (Conrath, 2011; Kohler et al., 2002; Martinez-Medina et al., 2016). To analyze the priming effect, OGs and fl22 were sprayed on adult *det3* plants and after 24 h, the sprayed leaves were inoculated with *B. cinerea* spores. Before proceeding with the fungal inoculation, the expression of the late defense marker gene *PR1* was evaluated in the leaves of plants sprayed with the elicitors. The time-course analysis revealed that *PR1* expression was induced at comparable levels in wild-type and *det3* mutant plants at 16h post-elicitor treatment. However, the induction of PR1 expression was significantly reduced in *det3* mutant at 24h post-treatment with OGs, which coincided with the time of fungal inoculation (Supplementary Fig. S2).

As expected, wild-type plants pre-treated with OGs or flg22 exhibited reduced susceptibility compared to non-pre-treated plants. Surprisingly, compared to the wild type, both elicitor pre-treatments increased susceptibility to fungal infection in *det3* mutant plants, since lesion areas and disease symptoms were both increased in pathogen-inoculated elicitor-pretreated leaves (Fig. 3d–i). These results clearly indicate that the higher basal resistance to *B. cinerea* displayed by the *det3* mutant was completely reversed by the pre-treatment with either OGs or flg22, although these elicitors were both able to induce a primed state in the same plant (Supplementary Fig. S2).

3.4. Fluorescently labelled OGs are internalized by endocytosis only in the root cells of wild type seedlings

Since the V-ATPase activity in the TGN is required for endocytic and secretory trafficking (Brux et al., 2008; Seidel, 2022), we investigated the role of endocytic pathway in OG signaling and whether the *det3* mutant shows any defects related to this function.

Alexa Fluor 488 labelled OGs (AF-OGs) were prepared, and their elicitor activity was confirmed by analysing the induction of *FOX1* gene in AF-OG-treated plants by qRT-PCR (Supplementary Fig. S3). Using confocal microscopy (CM), we observed their cellular distribution in roots of treated seedlings. To test the specificity of the fluorescent OG uptake, the fluorochrome AF alone was used as controls in a parallel assay (Supplementary Fig. S4a). While the early distribution of the two types of fluorescent molecules (AF and AF-OGs) at the level of the cell wall was not significantly different, only AF-OGs were observed within the cells after 30 min (Supplementary Fig. S4b). The AF-OGs first accumulated at the level of the cell wall and in proximity to the cell surface and then appeared in small vesicles, likely due to internalization through the endocytic pathway (Supplementary Fig. S4b). In the *det3* mutant, the internalization of AF-OGs was severely impaired, with much fewer vesicles and a more diffuse background labelling that made the treatments with AF and AF-OGs indistinguishable (Supplementary Figs. S4c and d). The AF-OGs uptake was also investigated through a co-localization analysis using FM4-64, a tracer commonly employed to study dynamic endocytic processes (Rigal et al., 2015). The high degree of co-localization between the FM4-64 signal and AF-OGs in wild type seedlings clearly indicated that AF-OGs were internalized through endocytic vesicles (Fig. 4a–c). Conversely, the uptake of AF-OGs in the *det3* mutant was significantly impaired (Fig. 4b–d). These observations indicate the involvement of the V-ATPases in the energy-dependent endocytic process of cell wall DAMPs and provide additional *in vivo* evidence for the internalization of OGs. In conclusion, these results indicate that V-ATPase activity is involved in OG signaling and, probably, in the mobilization/recycling of putative OGs-PRR complexes from cell surface.

4. Discussion

We show in this work that the subunit C of V-ATPase DET3 plays an important role in the response to both OGs and flg22.

V-ATPases, belonging to the hetero-oligomeric H + -pumps, consist of two structurally distinct domains (V0 and V1) and generate the membrane potential and proton motive force necessary for secondary active transport (Sze et al., 1992, 2002). V-ATPases are highly conserved proteins since they can be found in all eukaryotic cells (Beyenbach and Wieczorek, 2006; Schumacher and Krebs, 2010) where they are localized in the plasma membrane (animals), the tonoplast (plants) and

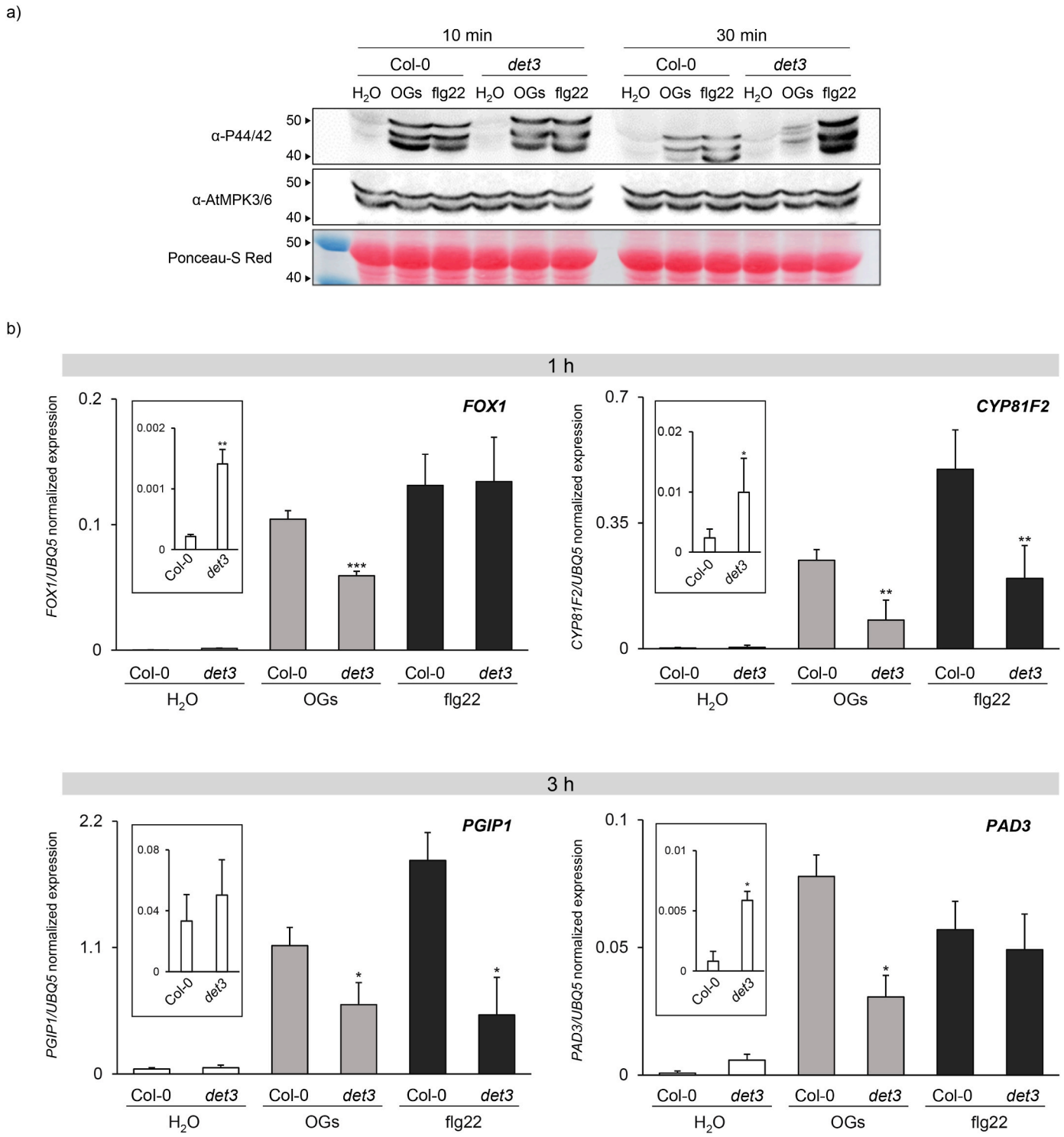

Fig. 2. Analysis of MAPK activation and defense marker gene induction in elicitor-treated wild-type and *det3* seedlings. a) Immunoblot analysis on MPK3/6 phosphorylation in response to OGs and flg22 elicitors. 10-day-old Col-0 and *det3* seedlings were treated for 10 and 30 min with OGs and flg22. Phosphorylated MPK3 and MPK6 (pMPK3/6) were detected by a α-phospho-p44/42 MAPK (Erk1/2) (Thr202/Tyr204) antibody. Total MPK3 and MPK6 were detected using α-AtMAPK3/6 antibodies. Ponceau-S Red staining was used to verify the equal loading. The experiment was repeated three times with similar results. b) Expression of the defense marker genes determined by qRT-PCR in 10-day-old of Col-0 and *det3* seedlings upon 1 h- and 3 h-treatment with H_2O, OGs and flg22. Normalization of gene expression was performed by using *UBQ5* a reference. Values are means of three independent biological experiments. Bars represent mean ± SD (n = 3). Inset indicate transcript levels in the water-treated seedlings. Asterisks indicate statistically significant differences between WT and *det3* mutants, according to Student's t-test (*, $p < 0.05$; **, $p < 0.01$; ***, $p < 0$ 0.001).

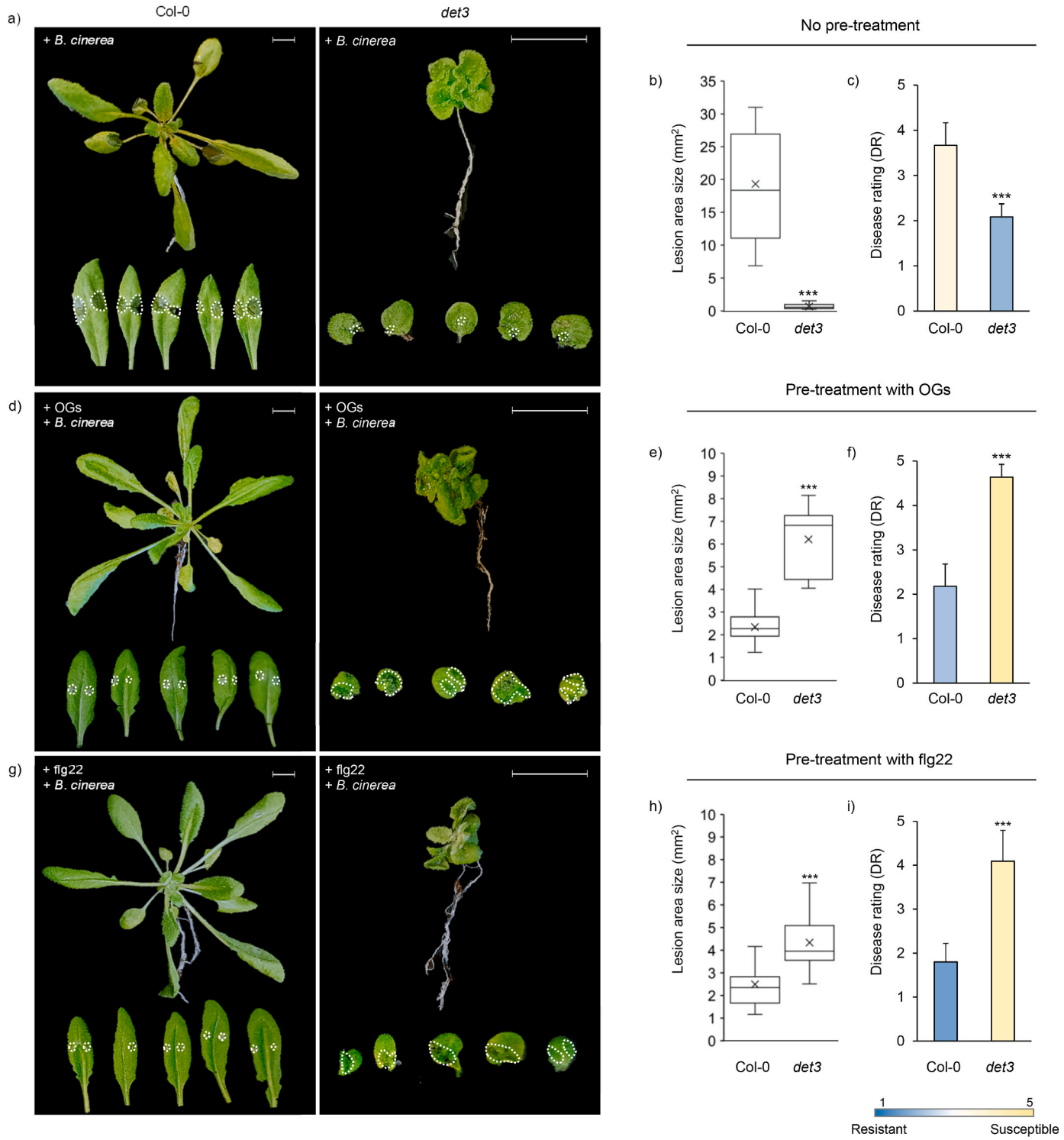

Fig. 3. Impact of *det3* mutation on basal and elicitor-induced resistance against *B. cinerea*. Infection assay on leaves of four-week-old Col-0 and *det3* plants. a) Representative images of Col-0 and *det3* plants/leaves infected with *B. cinerea*, (b) lesion areas (mm^2) of infected leaves and (c) DR rating at 48 h post infection with *B. cinerea*. d-f) Infection assay on leaves of four-week-old Col-0 and *det3* plants sprayed with OGs 24 h before the infection. d) Representative images of Col-0 and *det3* plants/leaves infected with *B. cinerea*, (e) lesion areas (mm^2) of infected leaves and (f) DR rating at 48 h post infection with *B. cinerea*. g-i) Infection assay on leaves of four-week-old Col-0 and *det3* plants sprayed with flg22 24 h before the infection. g) Representative images of Col-0 and *det3* plants/leaves infected with *B. cinerea*, (h) lesion areas (mm^2) of infected leaves and (i) DR rating at 48 h post infection with *B. cinerea*. Each lesion area is delimited on the leaf surface by a white dotted line. DR rating ranges from 1 (non-infected plants) to 5 (dead plants). The color-coding of each column indicates the level of the observed resistance phenotype, i.e., from susceptible (yellow) to resistant (blue). Data are means ± SE (n > 10); asterisks indicate statistically significant differences between wild-type and *det3* mutant according to Student's t-test (**, $p > 0.01$; ***, $p < 0.001$). The experiments were repeated twice with similar results. Scale bars = 10 mm.

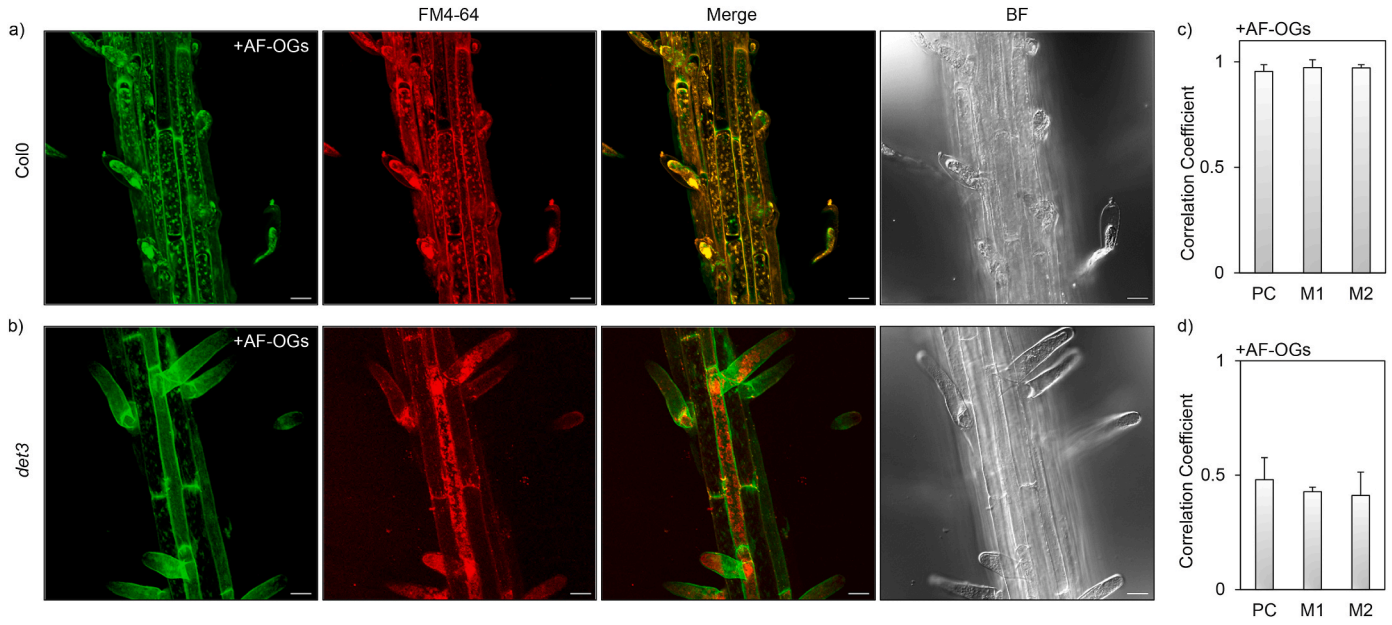

Fig. 4. Confocal microscopy analysis of wild type and *det3* roots upon treatment with AF-OGs. Confocal microscope analysis of roots from seven-days old Col0 (a) and *det3* (b) seedlings after 30 min of treatment with (a, b) Alexa Fluor 488-labelled OGs (AF-OGs) and FM4-64 labelling (FM4-64). AF-OGs, green; FM4-64, red; merged channels, orange. The corresponding bright-field (BF) microscopy images are shown. Scale bar = 20 μm. c,d) For each genotype, the degree of colocalization between the green and red channels was expressed with Pearson's correlation coefficient (PC) and the Mander's colocalization coefficients M1 and M2. c) M1 represents the fraction of AF-OGs (green signal) overlapping with the tracer FM4-64 (red signal) in Col0 seedlings whereas M2 represents the fraction of FM4-64 (red signal) overlapping with the fraction of AF-OGs (green signal) in the same genetic background. d) M1 represents the fraction of AF-OGs (green signal) overlapping with the tracer FM4-64 (red signal) in *det3* seedlings whereas M2 represents the fraction of FM4-64 (red signal) overlapping with the fraction of AF-OGs (green signal) in the same genetic background. [PC = 0, non-colocalization; PC = 1, complete colocalization].

endomembrane compartments characterized by a secretory trafficking pathway (fungi, plants and animals), such as the TGN/EE, a dynamic organelle responsible for receiving and sorting proteins to different subcellular destinations (Allen et al., 2000; Dettmer et al., 2006; Luo et al., 2015; Viotti et al., 2010). Changes in pH and uphill transport of protons mediated by V-ATPases have a relevant role not only in pH homeostasis of cell, but also in endomembrane trafficking and post-translational processing of secretory proteins, in both plants (Robinson et al., 2012) and animals (Huotari and Helenius, 2011). The fact that only a knock-down mutant, i.e., the *det3* mutant used in this study, has been identified suggests that the total loss of its function is lethal for plants (Schumacher et al., 1999); this conclusion is supported by the severe growth alterations displayed by the mutant (Supplementary Fig. S1b).

In basal conditions, the growth medium of *det3* mutant seedlings exhibited a higher pH value of 6.2 compared to that of wild-type plants (Fig. 1a). In this regard, it is interesting to note that, although mammalian V-ATPases have been found on the plasma membrane in specialized cells (Emruli et al., 2016), such a localization has never been shown in plant cells. Instead, V-ATPases have been found in the tonoplast and the TGN/EE, suggesting that perturbed intracellular pH homeostasis caused by the loss of DET3 may have effects, directly or indirectly, on extracellular pH homeostasis, making it more alkaline. It's worth noting that the V-ATPase overexpression has been observed in several human tumors, where it has been demonstrated to increase the extracellular acidification (Emruli et al., 2016).

However, in the medium of liquid-grown seedlings, the extracellular alkalinization induced by treatment with flg22 and OGs was less pronounced in the *det3* mutant than in wild-type plants, ultimately reaching a pH value only slightly higher (of about 0.3 pH units) than that observed in the wild type. It is not known if homeostatic mechanisms, independent of DET3, prevent excessive alkalinization of the extracellular medium in response to elicitors. It is known that OGs induce phosphorylation of plasma membrane H + -ATPases AHA1 and AHA2 (Mattei et al., 2016), a modification reported to inhibit proton transport and that may contribute to the extracellular alkalinization induced by elicitors (Fuglsang and Palmgren, 2021). The activity of plasma membrane proton pumps may already be partially inhibited in the *det3* mutant, consistent with the higher basal pH. Subsequent elicitation may result in complete inactivation of these pumps, ultimately bringing the pH to a level comparable as that observed in the wild type after elicitation. Also, other mechanisms responsible for alkalinization, such as proton-coupled anion symport, cannot be excluded (Boller and Felix, 2009; Elmore and Coaker, 2011; Jeworutzki et al., 2010).

Both OG- and flg22-induced ROS production was increased in *det3* mutant seedlings, indicating that the partial loss of DET3 increased the extracellular H_2O_2 accumulation (Fig. 1c and d). It is possible that the pH condition of the extracellular environment, which is altered in the *det3* mutant, influences the activity of the ROS-generating enzyme, or alternatively that these enzymes are de-regulated in the mutants through more complex transcriptional or post-transcriptional mechanisms.

We also observed a relevant reduction of OG-induced MPK3 and MPK6 phosphorylation, whereas, in accordance with previous observations (Keinath et al., 2010), an increased phosphorylation was observed in *det3* mutant 30 min after treatment with flg22. Notably, an opposite effect on MAPK phosphorylation similar to that in the *det3* mutant in response to treatments with OGs and a bacterial PAMP (elf18) has been observed in conditional triple mutants defective in the MAPKKKs known as ANPs, which also show severe developmental defects (Savatin et al., 2014).

Consistent with the reduced phosphorylation of MPK3 and MPK6, a reduced induction of the expression of defense marker genes *FOX1*, *CYP81F2*, *PGIP1* and *PAD3* was observed after 1 and 3 h of treatment with OGs (Fig. 2). On the other hand, despite the increased flg22-induced phosphorylation of MPK3 and MPK6 in the *det3* mutant flg22-induced expression of *FOX1* and *PAD3* was not significantly affected compared to WT plant (Fig. 2). Noteworthy, the higher basal expression

of *FOX1*, *CYP81F2* and *PAD3* in the *det3* mutant may be more likely ascribed to a generic stress response derived from the altered developmental phenotype rather than to the specific absence of DET3 function (Fig. 2b). It has also been noted that the direction of the changes in the accumulation of H_2O_2 in response to OGs shows no correlation with the changes in the MAPK phosphorylation.

Compared to wild type plants, *det3* mutant plants were significantly more resistant against *B. cinerea* infection (Fig. 3a–c). The enhanced basal resistance may be attributed to one or more constitutive feature of *det3* mutant, including an altered cell wall composition characterized by an increased abundance of glucuronoxylans and xyloglucans, with a reduced presence of pectic uronic acids (Molina et al., 2021). This atypical cell wall composition could hinder efficient colonization of plant tissue by the fungus. Moreover, the altered pH homeostasis of *det3*, which results in a more alkaline extracellular pH, may also play a role, since acidification of the tissue by *B. cinerea* is required for the proper progression of the infection (Muller et al., 2018).

The OG-induced dephosphorylation of the C subunit of the V-ATPase (DET3) is expected to have an important impact of the function of the holoenzyme. The activity of eukaryotic V-ATPase is known to be regulated by (i) the reversible assembly/disassembly of V0-V1 domains (Voss et al., 2007) and (ii) the activity of specific kinases that, in turn, influences the assembly, activation, and function of the V-ATPase holoenzyme. However, differently from yeast and mammalian V-ATPases, the regulation by reversible assembly/disassembly may not be conserved in plants (Seidel, 2022) and, additionally, the role of phosphorylation and dephosphorylation dynamics in regulating plant V-ATPase orthologs remains poorly understood. So far only the Arabidopsis WNK8 serine/threonine kinase, member of the WNK family, which is distinguished by an unusual positioning of a catalytic lysine thus earning the acronym "WITH NO LYSINE", has been characterized as capable of phosphorylating DET3 (Cao-Pham et al., 2018; Hong-Hermesdorf et al., 2006). The *det3* default status may mimic the condition, i.e. dephosphorylation, determined by the perception of OGs that likely contributes to switching cell activity towards plant defense and inhibiting plant growth and development. This might explain the strong basal resistance to *B. cinerea*.

Instead, the observation that OG-pre-treatment is detrimental for the ability of the *det3* mutant to combat *B. cinerea* is puzzling. An increased susceptibility induced by elicitor pre-treatment has never been described. The priming effect was evaluated by analyzing the induction over time of the late-defense marker gene PR1 in plant leaves sprayed with OGs and flg22 before fungal inoculation. The induction of PR1 expression was significantly reduced in the *det3* mutant at 24 h post-treatment with OGs, which coincided with the time of fungal inoculation. This result suggests a compromised ability of the det3 mutant to maintain a primed state over time, leading to a weaker defense response when the plant is later exposed to the fungal pathogen. The impairment in elicitor-induced protection indicates that the *det3* mutant not only lacks the mechanisms necessary to efficiently counter the invading fungus but also shows a suppression of its constitutive defense potential (Fig. 3d–i). In this regard, the higher H_2O_2 accumulation of *det3* mutant in response to elicitors (Fig. 1c and d) may also contribute to the increased susceptibility to *B. cinerea*. It is known that the fungus itself generates ROS and H_2O_2 during infection (Rolke et al., 2004); for example, it generates ROS directly from its hyphal tips in order to accumulate H_2O_2 inside and around the penetrated cell walls (Tenberge et al., 2002). The production of ROS has been observed to correlate with susceptibility to necrotrophic pathogens, such as *B. cinerea*, in different Arabidopsis mutants (Veronese et al., 2006; Wang et al., 2009). Moreover, increased levels of ROS, observed in plants silenced in the tomato histone H2B mono-ubiquitination enzymes SlHUB1 and SlHUB2, were associated with an increased susceptibility to *B. cinerea* (Zhang et al., 2015). Therefore, the exaggerated H_2O_2 accumulation in the elicitor-treated *det3* mutant plants may provide a more ideal environment for the virulence of the fungus. Taken together, our findings support the hypothesis that necrotrophic fungi like *B. cinerea* depend significantly on the direct or indirect generation of ROS to invade host tissues.

We uncover here an additional feature of the *det3* mutant, namely its reduced capability to internalize fluorescently labelled OGs. In the roots of wild-type plants, OG fluorescence was primarily observed at the cell surface within a few minutes, followed by its appearance in vesicles inside the cell, indicating rapid endocytosis. This process was clearly impaired in the mutant.

Endocytosis facilitated by receptor-ligand interactions has been documented for OGs in cultured soybean cells (Horn et al., 1989). Furthermore, the uptake of pectin fragments and their integration into the developing cell plate during cytokinesis has been reported (Dhonukshe et al., 2006; Samaj et al., 2005). More recently, the interaction of OGs with Rapid Alkalinization Factor 1 (RALF1) has been shown to promote the clustering and endocytosis of membrane protein condensates formed by Feronia (FER) and Lorelei-Like-GPI-anchored protein 1 (LLG1). Importantly, the reduced internalization of such protein aggregates in the OG-treated *ralf1* mutant was associated with a weaker OG-triggered immune response (Liu et al., 2024).

The uptake of AF-OGs was investigated through a co-localization analysis using FM4-64: in wild-type seedlings, there was a high degree of co-localization between the FM4-64 signal and AF-OGs, clearly indicating that AF-OGs were internalized via endocytic vesicles (Fig. 4a–c). Conversely, in the *det3* mutant, the uptake of AF-OGs was significantly impaired (Fig. 4b–d). This impairment indicates a disruption in the endocytic process, due to the defective function of the DET3 protein.

The DET3 gene is involved in vesicle trafficking, and its mutation likely impairs the cells' ability to internalize OGs efficiently. This impairment aligns with the observed defect in the priming response in the det3 mutant, underscoring that proper internalization and signaling of OGs are crucial for initiating and maintaining a primed state in plant defense responses. Therefore, the impaired endocytosis of OGs in the det3 mutant provides a mechanistic explanation for its compromised immune priming, indicating that the effectiveness of OG-triggered immune response depends not only on the recognition of OGs but also on their efficient internalization.

Moreover, the internalization of OGs can contribute to remove the residual elicitor-active molecules from the cell surface, thereby clearing the stimulus that promoted the reallocation of metabolic energy from primary to secondary metabolism (Horn et al., 1989). This likely represents an additional homeostatic mechanism, beside that based on enzymatic oxidation of OGs, catalyzed by specific plant oligosaccharide oxidases belonging to BBE-l protein family, and capable of impairing the elicitor activity of such DAMPs (Benedetti et al., 2018; Costantini et al., 2023; Locci et al., 2019).

5. Conclusions

Our observations highlight that the *det3* mutant, which exhibits impairments in the endocytosis pathway and rapid internalization of OGs, also shows defects in defense responses to OGs, including extracellular alkalinization, MAPK phosphorylation and early defense gene induction. These findings suggest a close association between OG internalization and their action, indicating that the V-ATPase function is essential for both the early activation of the signal cascade by OGs and potentially their clearance. Overall, our results indicate that not only is MAMP signaling compromised, but also DAMP signaling is severely impaired in the *det3* mutant uncovering the crucial role of V-ATPase in both the early responses induced by OGs and their internalization.

CRediT authorship contribution statement

B.M. and G.D.L. conceived the project. M.G. designed and performed the experiments. V.S. and R.P. contributed to perform the experiments. M.G., M.B., G.D.L. and B.M. analyzed the data. M.B., G.D.L., M.G., M.B.

and R.P. wrote the manuscript draft. M.B., G.D.L. and B.M. wrote the manuscript in its final version. B.M. supervised the research. All the authors have approved the final manuscript.

Declaration of competing interest

The authors declare that they have no known competing financial interests or personal relationships that could have appeared to influence the work reported in this paper.

Data availability

No data was used for the research described in the article.

Acknowledgment

The authors gratefully acknowledge Prof. Ralph Panstruga (Institute for Biology I of RWTH Aachen University, Germany) for kindly providing the seeds of *det3* mutant, Dr. Jozef Mravec (Department of Plant and Environmental Sciences, University of Copenhagen, Denmark) for helpful suggestions in the preparation of AF-OGs, and the Microscopy Centre (Microscopy Centre (University of L'Aquila, Italy) for support and assistance in confocal microscopy analysis.

This work was supported by the Italian Ministry of Education, University and Research (PRIN 2017ZBBYNC and PRIN 2022WLZ4HB) funded to G.D.L. and B.M.

Appendix A. Supplementary data

Supplementary data to this article can be found online at https://doi.org/10.1016/j.plaphy.2024.109117.

References

Allen, G.J., Chu, S.P., Schumacher, K., Shimazaki, C.T., Vafeados, D., Kemper, A., Schroeder, J.I., 2000. Alteration of stimulus-specific guard cell calcium oscillations and stomatal closing in Arabidopsis det3 mutant. Science 289 (5488), 2338–2342.

Asai, T., Tena, G., Plotnikova, J., Willmann, M.R., Chiu, W.L., Gomez-Gomez, L., Sheen, J., 2002. MAP kinase signalling cascade in Arabidopsis innate immunity. Nature 415 (6875), 977–983. https://doi.org/10.1038/415977a.

Barrett, L.G., Heil, M., 2012. Unifying concepts and mechanisms in the specificity of plant-enemy interactions. Trends Plant Sci. 17 (5), 282–292.

Benedetti, M., Verrascina, I., Pontiggia, D., Locci, F., Mattei, B., De Lorenzo, G., Cervone, F., 2018. Four Arabidopsis berberine bridge enzyme-like proteins are specific oxidases that inactivate the elicitor-active oligogalacturonides. Plant J. 94 (2), 260–273. https://doi.org/10.1111/tpj.13852.

Bethke, G., Pecher, P., Eschen-Lippold, L., Tsuda, K., Katagiri, F., Glazebrook, J., Lee, J., 2012. Activation of the Arabidopsis thaliana mitogen-activated protein kinase MPK11 by the flagellin-derived elicitor peptide, flg22. Mol. Plant Microbe Interact. 25 (4), 471–480.

Beyenbach, K.W., Wieczorek, H., 2006. The V-type H+ ATPase: molecular structure and function, physiological roles and regulation. J. Exp. Biol. 209 (Pt 4), 577–589. https://doi.org/10.1242/jeb.02014.

Boller, T., Felix, G., 2009. A renaissance of elicitors: perception of microbe-associated molecular patterns and danger signals by pattern-recognition receptors. Annu. Rev. Plant Biol. 60, 379–406.

Bolwell, G.P., Bindschedler, L.V., Blee, K.A., Butt, V.S., Davies, D.R., Gardner, S.L., Minibayeva, F., 2002. The apoplastic oxidative burst in response to biotic stress in plants: a three-component system. J. Exp. Bot. 53 (372), 1367–1376.

Boudsocq, M., Willmann, M.R., McCormack, M., Lee, H., Shan, L., He, P., Sheen, J., 2010. Differential innate immune signalling via Ca^{2+} sensor protein kinases. Nature 464 (7287), 418–422. https://doi.org/10.1038/nature08794.

Brux, A., Liu, T.Y., Krebs, M., Stierhof, Y.D., Lohmann, J.U., Miersch, O., Schumacher, K., 2008. Reduced V-ATPase activity in the trans-Golgi network causes oxylipin-dependent hypocotyl growth inhibition in Arabidopsis. Plant Cell 20 (4), 1088–1100.

Cabrera y Poch, H.L., Peto, C.A., Chory, J., 1993. A mutation in the Arabidopsis DET3 gene uncouples photoregulated leaf development from gene expression and chloroplast biogenesis. Plant J. 4 (4), 671–682. https://doi.org/10.1046/j.1365-313X.1993.04040671.x.

Cao-Pham, A.H., Urano, D., Ross-Elliott, T.J., Jones, A.M., 2018. Nudge-nudge, WNK-WNK (kinases), say no more? New Phytol. 220 (1), 35–48. https://doi.org/10.1111/nph.15276.

Cervone, F., De Lorenzo, G., D'Ovidio, R., Hahn, M.G., Ito, Y., Darvill, A., Albersheim, P., 1989. Phytotoxic effects and phytoalexin-elicitor activity of microbial pectic enzymes. In: Graniti, A., Durbin, R.D., Ballio, A. (Eds.), Phytotoxins and Plant Pathogenesis, NATO ASI Series, H27. Springer Verlag, pp. 473–477. https://doi.org/10.1007/978-3-642-73178-5_63.

Chisholm, S.T., Coaker, G., Day, B., Staskawicz, B.J., 2006. Host-microbe interactions: shaping the evolution of the plant immune response. Cell 124 (4), 803–814. https://doi.org/10.1016/j.cell.2006.02.008.

Conrath, U., 2011. Molecular aspects of defence priming. Trends Plant Sci. 16 (10), 524–531. https://doi.org/10.1016/j.tplants.2011.06.004.

Costantini, S., Benedetti, M., Pontiggia, D., Giovannoni, M., Cervone, F., Mattei, B., De Lorenzo, G., 2023. Berberine bridge enzyme-like oxidases of cellodextrins and mixed-linked β-glucans control seed coat formation. Plant Physiol. https://doi.org/10.1093/plphys/kiad457.

De Lorenzo, G., Brutus, A., Savatin, D.V., Sicilia, F., Cervone, F., 2011. Engineering plant resistance by constructing chimeric receptors that recognize damage-associated molecular patterns (DAMPs). FEBS (Fed. Eur. Biochem. Soc.) Lett. 585 (11), 1521–1528. https://doi.org/10.1016/j.febslet.2011.04.043.

De Lorenzo, G., D'Ovidio, R., Cervone, F., 2001. The role of polygalacturonase-inhibiting proteins (PGIPS) in defense against pathogenic fungi. Annu. Rev. Phytopathol. 39, 313–335. https://doi.org/10.1146/annurev.phyto.39.1.313.

Denoux, C., Galletti, R., Mammarella, N., Gopalan, S., Werck, D., De Lorenzo, G., Dewdney, J., 2008. Activation of defense response pathways by OGs and Flg22 elicitors in Arabidopsis seedlings. Mol. Plant 1 (3), 423–445. https://doi.org/10.1093/mp/ssn019.

Dettmer, J., Hong-Hermesdorf, A., Stierhof, Y.D., Schumacher, K., 2006. Vacuolar H+-ATPase activity is required for endocytic and secretory trafficking in Arabidopsis. Plant Cell 18 (3), 715–730.

Dhonukshe, P., Baluska, F., Schlicht, M., Hlavacka, A., Samaj, J., Friml, J., Gadella Jr., T. W., 2006. Endocytosis of cell surface material mediates cell plate formation during plant cytokinesis. Dev. Cell 10 (1), 137–150.

Elmore, J.M., Coaker, G., 2011. The role of the plasma membrane H+-ATPase in plant-microbe interactions. Mol. Plant 4 (3), 416–427.

Emruli, V.K., Olsson, R., Ek, F., Ek, S., 2016. Identification of V-ATPase as a molecular sensor of SOX11-levels and potential therapeutic target for mantle cell lymphoma. BMC Cancer 16, 493. https://doi.org/10.1186/s12885-016-2550-4.

Fabian, M., Gao, M., Zhang, X., Shi, J., Vrydagh, L., Kim, S., Lu, H., 2023. The flowering time regulator FLK controls pathogen defense in Arabidopsis thaliana. Plant Physiol. 191 (4) https://doi.org/10.1093/plphys/kiad021.

Ferrari, S., Galletti, R., Denoux, C., De Lorenzo, G., Ausubel, F.M., Dewdney, J., 2007. Resistance to *Botrytis cinerea* induced in Arabidopsis by elicitors is independent of salicylic acid, ethylene, or jasmonate signaling but requires PHYTOALEXIN DEFICIENT3. Plant Physiol. 144 (1), 367–379. https://doi.org/10.1104/pp.107.095596.

Ferrari, S., Plotnikova, J.M., De Lorenzo, G., Ausubel, F.M., 2003. Arabidopsis local resistance to Botrytis cinerea involves salicylic acid and camalexin and requires EDS4 and PAD2, but not SID2, EDS5 or PAD4. Plant J. 35 (2), 193–205. https://doi.org/10.1046/j.1365-313X.2003.01794.x.

Fuglsang, A.T., Palmgren, M., 2021. Proton and calcium pumping P-type ATPases and their regulation of plant responses to the environment. Plant Physiol. 187 (4), 1856–1875. https://doi.org/10.1093/plphys/kiab330.

Fukao, Y., Ferjani, A., 2011. V-ATPase dysfunction under excess zinc inhibits Arabidopsis cell expansion. Plant Signal. Behav. 6 (9), 1253–1255. https://doi.org/10.4161/psb.6.9.16529.

Galletti, R., Denoux, C., Gambetta, S., Dewdney, J., Ausubel, F.M., De Lorenzo, G., Ferrari, S., 2008. The AtrbohD-mediated oxidative burst elicited by oligogalacturonides in Arabidopsis is dispensable for the activation of defense responses effective against *Botrytis cinerea*. Plant Physiol. 148 (3), 1695–1706. https://doi.org/10.1104/pp.108.127845.

Galletti, R., Ferrari, S., De Lorenzo, G., 2011. Arabidopsis MPK3 and MPK6 play different roles in basal and oligogalacturonide- or flagellin-induced resistance against Botrytis cinerea. Plant Physiol. 157 (2), 804–814. https://doi.org/10.1104/pp.111.174003.

Geilfus, C.M., 2017. The pH of the apoplast: dynamic factor with functional impact under stress. Mol. Plant 10 (11), 1371–1386. https://doi.org/10.1016/j.molp.2017.09.018.

Giovannoni, M., Larini, I., Scafati, V., Scortica, A., Compri, M., Pontiggia, D., Mattei, B., 2021a. A novel Penicillium sumatraense isolate reveals an arsenal of degrading enzymes exploitable in algal bio-refinery processes. Biotechnol. Biofuels 14 (1), 180. https://doi.org/10.1186/s13068-021-02030-9.

Giovannoni, M., Lironi, D., Marti, L., Paparella, C., Vecchi, V., Gust, A.A., Ferrari, S., 2021b. The *Arabidopsis thaliana* LysM-containing Receptor-Like Kinase 2 is required for elicitor-induced resistance to pathogens. Plant Cell Environ. 44 (12), 3545–3562. https://doi.org/10.1111/pce.14192.

Giovannoni, M., Marti, L., Ferrari, S., Tanaka-Takada, N., Maeshima, M., Ott, T., Mattei, B., 2021c. The plasma membrane-associated Ca^{2+}- binding protein PCaP1 is required for oligogalacturonide and flagellin-induced priming and immunity. Plant Cell Environ. 44 (9), 3078–3093. https://doi.org/10.1111/pce.14118.

Gravino, M., Locci, F., Tundo, S., Cervone, F., Savatin, D.V., De Lorenzo, G., 2017. Immune responses induced by oligogalacturonides are differentially affected by AvrPto and loss of BAK1/BKK1 and PEPR1/PEPR2. Mol. Plant Pathol. 18 (4), 582–595. https://doi.org/10.1111/mpp.12419.

Hahn, M.G., 1981. Fragments of Plant and Fungal Cell Wall Polysaccharides Elicit the Accumulation of Phytoalexins in Plants. University of Colorado. Ph.D. Thesis.

Hong-Hermesdorf, A., Brux, A., Gruber, A., Gruber, G., Schumacher, K., 2006. A WNK kinase binds and phosphorylates V-ATPase subunit C. FEBS (Fed. Eur. Biochem. Soc.) Lett. 580 (3), 932–939. https://doi.org/10.1016/j.febslet.2006.01.018.

Horn, M.A., Heinstein, P.F., Low, P.S., 1989. Receptor-mediated endocytosis in plant cells. Plant Cell 1, 1003–1009.

Huffaker, A., Pearce, G., Ryan, C.A., 2006. An endogenous peptide signal in Arabidopsis activates components of the innate immune response. Proc. Natl. Acad. Sci. USA 103.
Huotari, J., Helenius, A., 2011. Endosome maturation. EMBO J. 30 (17), 3481–3500.
Ichimura, K., Tena, G., Sheen, J., Henery, Y., Champion, A., Kreis, M., Zhang, S., Hirt, H., Wilson, C., Ellis, B.E., 2002. Mitogen-activated protein kinase cascades in plants: a new nomenclature. Trends Plant Sci. 7 (7) https://doi.org/10.1016/s1360-1385(02)02302-6.
Jeworutzki, E., Roelfsema, M.R., Anschütz, U., Krol, E., Elzenga, J.T., Felix, G., Becker, D., 2010. Early signaling through the Arabidopsis pattern recognition receptors FLS2 and EFR involves Ca-associated opening of plasma membrane anion channels. Plant J. 62 (3), 367–378. https://doi.org/10.1111/j.1365-313X.2010.04155.x.
Jiang, Z.Y., Woollard, A.C., Wolff, S.P., 1990. Hydrogen peroxide production during experimental protein glycation. FEBS (Fed. Eur. Biochem. Soc.) Lett. 268 (1), 69–71.
Keinath, N.F., Kierszniowska, S., Lorek, J., Bourdais, G., Kessler, S.A., Shimosato-Asano, H., Panstruga, R., 2010. PAMP (Pathogen-associated molecular pattern)-induced changes in plasma membrane compartmentalization reveal novel components of plant immunity. J. Biol. Chem. 285 (50), 39140–39149.
Kohler, A., Schwindling, S., Conrath, U., 2002. Benzothiadiazole-induced priming for potentiated responses to pathogen infection, wounding, and infiltration of water into leaves requires the NPR1/NIM1 gene in Arabidopsis. Plant Physiol. 128 (3), 1046–1056.
Liu, M.J., Yeh, F.J., Yvon, R., Simpson, K., Jordan, S., Chambers, J., Cheung, A.Y., 2024. Extracellular pectin-RALF phase separation mediates FERONIA global signaling function. Cell 187 (2), 312–330 e322. https://doi.org/10.1016/j.cell.2023.11.038.
Locci, F., Benedetti, M., Pontiggia, D., Citterico, M., Caprari, C., Mattei, B., De Lorenzo, G., 2019. An Arabidopsis berberine bridge enzyme-like protein specifically oxidizes cellulose oligomers and plays a role in immunity. Plant J. 98 (3), 540–554. https://doi.org/10.1111/tpj.14237.
Luo, Y., Scholl, S., Doering, A., Zhang, Y., Irani, N.G., Rubbo, S.D., Russinova, E., 2015. V-ATPase activity in the TGN/EE is required for exocytosis and recycling in Arabidopsis. Nat. Plants 1, 15094. https://doi.org/10.1038/nplants.2015.94.
Martinez-Medina, A., Flors, V., Heil, M., Mauch-Mani, B., Pieterse, C.M.J., Pozo, M.J., Conrath, U., 2016. Recognizing plant defense priming. Trends Plant Sci. 21 (10), 818–822. https://doi.org/10.1016/j.tplants.2016.07.009.
Mattei, B., Spinelli, F., Pontiggia, D., De Lorenzo, G., 2016. Comprehensive analysis of the membrane phosphoproteome regulated by oligogalacturonides in *Arabidopsis thaliana*. Front. Plant Sci. 7, 1107. https://doi.org/10.3389/fpls.2016.01107.
Molina, A., Miedes, E., Bacete, L., Rodríguez, T., Mélida, H., Denancé, N., Goffner, D., 2021. Cell wall composition determines disease resistance specificity and fitness. Proc. Natl. Acad. Sci. USA 118 (5), e2010243118. https://doi.org/10.1073/pnas.2010243118.
Mravec, J., Kracun, S.K., Rydahl, M.G., Westereng, B., Miart, F., Clausen, M.H., Willats, W.G., 2014. Tracking developmentally regulated post-synthetic processing of homogalacturonan and chitin using reciprocal oligosaccharide probes. Development 141 (24), 4841–4850.
Muller, N., Leroch, M., Schumacher, J., Zimmer, D., Konnel, A., Klug, K., Hahn, M., 2018. Investigations on VELVET regulatory mutants confirm the role of host tissue acidification and secretion of proteins in the pathogenesis of Botrytis cinerea. New Phytol. 219 (3), 1062–1074. https://doi.org/10.1111/nph.15221.
Nafisi, M., Goregaoker, S., Botanga, C., Glawischnig, E., Olsen, C., Halkier, B., Glazebrook, J., 2007. Arabidopsis cytochrome P450 monooxygenase 71A13 catalyzes the conversion of indole-3-acetaldoxime in camalexin synthesis. Plant Cell 19 (6). https://doi.org/10.1105/tpc.107.051383.
Ngou, B.P., Wyler, M., Schmid, M.W., Kadota, Y., Shirasu, K., 2024. Evolutionary trajectory of pattern recognition receptors in plants. Nat. Commun. 15 (308) https://doi.org/10.1038/s41467-023-44408-3.
Peiter, E., 2011. The plant vacuole: emitter and receiver of calcium signals. Cell Calcium 50 (2), 120–128. https://doi.org/10.1016/j.ceca.2011.02.002.
Pontiggia, D., Benedetti, M., Costantini, S., De Lorenzo, G., Cervone, F., 2020. Dampening the DAMPs: how plants maintain the homeostasis of cell wall molecular patterns and avoid hyper-immunity. Front. Plant Sci. 11, 613259 https://doi.org/10.3389/fpls.2020.613259.
Rajniak, J., Barco, B., Clay, N.K., Sattely, E.S., 2015. A new cyanogenic metabolite in Arabidopsis required for inducible pathogen defence. Nature 525 (7569), 376–379. https://doi.org/10.1038/nature14907.
Rasmussen, M.W., Roux, M., Petersen, M., Mundy, J., 2012. MAP kinase cascades in Arabidopsis innate immunity. Front. Plant Sci. 3, 169.
Rigal, A., Doyle, S.M., Robert, S., 2015. Live cell imaging of FM4-64, a tool for tracing the endocytic pathways in Arabidopsis root cells. Meth. Mol. Biol. 1242, 93–103 https://doi.org/10.1007/.
Robinson, D.G., Pimpl, P., Scheuring, D., Stierhof, Y.D., Sturm, S., Viotti, C., 2012. Trying to make sense of retromer. Trends Plant Sci. 17 (7), 431–439.
Rolke, Y., Liu, S., Quidde, T., Williamson, B., Schouten, A., Weltring, K., Tudzynski, P., 2004. Functional analysis of H(2)O(2)-generating systems in Botrytis cinerea: the major Cu-Zn-superoxide dismutase (BCSOD1) contributes to virulence on French bean, whereas a glucose oxidase (BCGOD1) is dispensable. Mol. Plant Pathol. 5 (1) https://doi.org/10.1111/j.1364-3703.2004.00201.x.
Ruijter, J.M., Pfaffl, M.W., Zhao, S., Spiess, A.N., Boggy, G., Blom, J., Vandesompele, J., 2013. Evaluation of qPCR curve analysis methods for reliable biomarker discovery: bias, resolution, precision, and implications. Methods 59 (1), 32–46. https://doi.org/10.1016/j.ymeth.2012.08.011.
Samaj, J., Read, N.D., Volkmann, D., Menzel, D., Baluska, F., 2005. The endocytic network in plants. Trends Cell Biol. 15 (8), 425–433.
Savatin, D.V., Gigli-Bisceglia, N., Marti, L., Fabbri, C., Cervone, F., De Lorenzo, G., 2014. The Arabidopsis NUCLEUS- AND PHRAGMOPLAST-LOCALIZED KINASE1-related protein kinases are required for elicitor-induced oxidative burst and immunity. Plant Physiol. 165 (3), 1188–1202. https://doi.org/10.1104/pp.114.236901.
Schumacher, K., Krebs, M., 2010. The V-ATPase: small cargo, large effects. Curr. Opin. Plant Biol. 13 (6), 724–730.
Schumacher, K., Vafeados, D., McCarthy, M., Sze, H., Wilkins, T., Chory, J., 1999. The Arabidopsis det3 mutant reveals a central role for the vacuolar H(+)-ATPase in plant growth and development. Gene Dev. 13 (24), 3259–3270. https://doi.org/10.1101/gad.13.24.3259.
Scortica, A., Giovannoni, M., Scafati, V., Angelucci, F., Cervone, F., De Lorenzo, G., Mattei, B., 2022. Berberine bridge enzyme-like oligosaccharide oxidases act as enzymatic transducers between microbial glycoside hydrolases and plant peroxidases. Mol. Plant Microbe Interact. https://doi.org/10.1094/MPMI-05-22-0113-TA.
Scortica, A., Scafati, V., Giovannoni, M., Benedetti, M., Mattei, B., 2023. Radical cation scavenging activity of berberine bridge enzyme-like oligosaccharide oxidases acting on short cell wall fragments. Sci. Rep. 13 (1), 4123. https://doi.org/10.1038/s41598-023-31335-y.
Seidel, T., 2022. The plant V-ATPase. Front. Plant Sci. 13, 931777 https://doi.org/10.3389/fpls.2022.931777.
Sze, H., Schumacher, K., Muller, M.L., Padmanaban, S., Taiz, L., 2002. A simple nomenclature for a complex proton pump: VHA genes encode the vacuolar H(+)-ATPase. Trends Plant Sci. 7 (4), 157–161. https://doi.org/10.1016/s1360-1385(02)02240-9.
Sze, H., Ward, J.M., Lai, S., 1992. Vacuolar H + -translocating ATPases from plants: structure, function, and isoforms. J. Bioenerg. Biomembr. 24, 371–381.
Szekeres, M., N,meth, K., Koncz-K lm n, Z., Mathur, J., Kauschmann, A., Altmann, T., Koncz, C., 1996. Brassinosteroids rescue the deficiency of CYP90, a cytochrome P450, controlling cell elongation and de-etiolation in arabidopsis. Cell 85 (2), 171–182.
Tang, R.J., Liu, H., Yang, Y., Yang, L., Gao, X.S., Garcia, V.J., Zhang, H.X., 2012. Tonoplast calcium sensors CBL2 and CBL3 control plant growth and ion homeostasis through regulating V-ATPase activity in Arabidopsis. Cell Res. 22 (12), 1650–1665. https://doi.org/10.1038/cr.2012.161.
Tenberge, K., Beckedorf, M., Schouten, B., Solf, M., Von den Driesch, M., 2002. In situ localization of AOS in host-pathogen interactions. Microsc. Microanal. 8 (S02), 250–251. https://doi.org/10.1017/S1431927602100067.
Tsuji, J., Jackson, E.P., Gage, D.A., Hammerschmidt, R., Somerville, S.C., 1992. Phytoalexin accumulation in Arabidopsis thaliana during the hypersensitive reaction to Pseudomonas syringae pv syringae. Plant Physiol. 98, 1304–1309.
Veronese, P., Nakagami, H., Bluhm, B., Abuqamar, S., Chen, X., Salmeron, J., Dietrich, R. A., Hirt, H., Mengiste, T., 2006. The membrane-anchored BOTRYTIS-INDUCED KINASE1 plays distinct roles in Arabidopsis resistance to necrotrophic and biotrophic pathogens. Plant Cell 18 (1), 257–273. https://doi.org/10.1105/tpc.105.035576.
Viotti, C., Bubeck, J., Stierhof, Y.D., Krebs, M., Langhans, M., van den Berg, W., Schumacher, K., 2010. Endocytic and secretory traffic in Arabidopsis merge in the trans-Golgi network/early endosome, an independent and highly dynamic organelle. Plant Cell 22 (4), 1344–1357. https://doi.org/10.1105/tpc.109.072637.
Voss, M., Vitavska, O., Walz, B., Wieczorek, H., Baumann, O., 2007. Stimulus-induced phosphorylation of vacuolar H(+)-ATPase by protein kinase A. J. Biol. Chem. 282 (46), 33735–33742. https://doi.org/10.1074/jbc.M703368200.
Wang, G., Seabolt, S., Hamdoun, S., Ng, G., Park, J., Lu, H., 2011. Multiple roles of WIN3 in regulating disease resistance, cell death, and flowering time in Arabidopsis. Plant Physiol. 156 (3) https://doi.org/10.1104/pp.111.176776.
Wang, X., Basnayake, B.M., Zhang, H., Li, G., Li, W., Virk, N., Mengiste, T., Song, F., 2009. The Arabidopsis ATAF1, a NAC transcription factor, is a negative regulator of defense responses against necrotrophic fungal and bacterial pathogens. Mol. Plant Microbe Interact. 22 (10), 1227–1238. https://doi.org/10.1094/MPMI-22-10-1227. PMID: 19737096.
Zhang, Y., Dong, C., 2007. Regulatory mechanisms of mitogen-activated kinase signaling. Cell. Mol. Life Sci. 64 (21), 2771–2789. https://doi.org/10.1007/s00018-007-7012-3.
Zhang, Y., Li, D., Zhang, H., Hong, Y., Huang, L., Liu, S., Song, F., 2015. Tomato histone H2B monoubiquitination enzymes SlHUB1 and SlHUB2 contribute to disease resistance against Botrytis cinerea through modulating the balance between SA- and JA/ET-mediated signaling pathways. BMC Plant Biol. 15 https://doi.org/10.1186/s12870-015-0614-2.

Appendix A Supplementary Material

The Vacuolar H^+-ATPase subunit C is involved in oligogalacturonide (OG) internalization and OG-triggered immunity.

Moira Giovannoni[1], Valentina Scafati[1], Renato Alberto Rodrigues Pousada[1], Manuel Benedetti[1], Giulia De Lorenzo[2], Benedetta Mattei[1,*]

[1]Department of Life, Health and Environmental Sciences, University of L'Aquila, 67100 L'Aquila, Italy

[2]Department of Biology and Biotechnology "C. Darwin", Sapienza University of Rome, 00185 Rome, Italy

*correspondence: mariabenedetta.mattei@univaq.it, Department of Life, Health and Environmental Sciences, University of L'Aquila, 67100 L'Aquila, Italy; phone +39 0862433256.

LIST OF CONTENT

Supplementary Data S1. Sequence analysis of *DET3*. In the *DET3* gene (AT1G12840), the bases corresponding to the start (ATG) and stop (TAA) codons are highlighted in green, the bases constituting the first intron are highlighted in yellow whereas the base T1592 is indicated in red. According to (Simpson et al., 1996), the two sequences “CTAAT” (in turquoise) and the distance from the 3^{l} splice junction indicate that the point mutation T1592A destroys a branchpoint consensus sequence. Compared to the wild-type plant, the point mutation T1592A resulted in 50% reduction of *DET3* expression in *det3* mutant (Schumacher et al., 1999).

AAGCGACTAAAGATCAGAAAGCATAAGAGGCACAATGGATTGAATTGCAAGAACATCAT
AGATATATATAAAGCCCACTTTGGTCCAAGCGTTTGAAACATCAATAGATATAACTAATAA
TCACTGAACAGTGACAAACTCTCTTTTAGAATCAAAGGAACTAATTCTCAGTTATCTTAA
TCACTAACCTCTTACAAGCTAAGGTCTTTAAGCATCACTATCACTGCTTTCATCATCCTC
GTCGTTGACATGGCGGTTACTGAATTCATTGGGGATGAAAACTCCAGGCTGGCTCGAT
CTTCTCCTAGTCCTCGACGGAAGGATATTATCCAAATCAACCTCAGCCAAAGGATCATC
GGAGAAATCGCTTTCGTCGTCTTCATCAAAACCTTCGTCATCTTCATCATCATCACTGT
CGTCTTCATCATCACTTTCTTCCACTTCGATCATTTTTCCCTTTCCCTTATCCTCTCGCG
AAATCCCTTTACCTTTCCTATCAACAACTTCTTCTTCTTCTTCTTCCTCGTCGTCTT
CCTCTTCATCTTCTTCATCCTCTTGCTCCTCTTCAGCTCCAACATCGCCGATTACGCCA
CTCTCAACCTCTTCAGCTGCTTTCTCCGATAAAACCGATGATTCTGCTCCAATCGTTTC
CTCGGTGGAAGAATTCAGATTCTCGATTTGGCCACTTCCATTAGTTTCTCCGTCTTTGG
ACTCAGAATCAGCAGAATTCAATGAAGGATTAAGCTTCTGAGCCTTGTTTGTCACATTA
TCCTGGTCTTGACAAAACAGATCCGATTTTCGCTTCACAGGAAACGAAGAATCCTGTT
GATTCTCAACATCCGCCATAGATGAATCAATCTTCTTACTTCAGAGACTCGCGATTTTG
GTTTGAGGACGACGATTCAGAGTTAGGGCTTTGAAGCTGAATCAAAACACTCGAGCCA
ATTTAGTTTGTAACCCTAGAAGTTTTTGTAGGGTTTTACCGTCTCTGTTTTTTATTATTTG
GATCTCTGAACACATTTGGCCCAGTATTAGCCCATTTACCTATCTTCTCAAAATATTTGG
TTCTTAACAAATTCAAGCCTAACCATTAGTACAATTTTAATTTTGATCTGTACATTTTCAAA
AACCGGACTCGAACCAAGATCAAATTCAACAATTGTGGCAATTTTAATGGTCGAGTCTC
CAGTGTGTATGTGGCAGTAGGAGAACGTGCCGGGGGATATTAAACCGGCTCAATGCTA
CAGTCGTACCGGTTTGTTTTTTTACTCGTTGGTATATAATTAAAACCGGTTATCCAATTTG
ACAGGCAGAGAGAAGAAGATTTGATTGAAGTACAGATCCATCGGAGAAGAAGACAGA
GAGATTGAAGATCAATGACTTCGAGATATTGGGTGGTGTCTCTTCCAGTGAAAGACTC
TGCTTCTTCGTTATGGAATCGATTACAAGAGCAGATCTCTAAGCATTCCTTTGATACTCC
AGTTTATCGGGTACTCTGATTTTTGCTCGATTTGGTCTTATTGCAAAATTTAGCACAGAT
CTTATACTATCTCTTGCTACTTTCGTGTCTACGATTCTAATTACGATCTAATTCCGTGAGT
TTTGGTTTCAATTTCGCAGTTTAACATTCCTAATCTTCGTGTTGGAACCTTAGATTCTCT
ACTCGCTCTCGGCGATGATCTGCTTAAGGTAAAATTCATTTGATCACTGAGTGGATTTT
ATGTTTTTGATTTTAAAATTCCTCTCTTGATTGAGAAATTTTTGAGATTTGTAGTCGAACA
GCTTTGTGGAAGGAGTTTCGCAAAAGATCAGGAGACAGATCGAAGAATTGGAGAGGA
TTTCTGGTGTTGAGAGCAACGCTCTTACAGTTGATGGAGTTCCTGTTGATTCTTATCTC
ACCAGGTATTTGTGATTTTCCGTCTCAGAAGGAGTTAATTGCTAATTTGGTGGTGATCG
AATTGTTAAAGAACGAAACTTTTGTTGATTGGTGGACTCAAGGTTTGTGTGGGATGAAG
CTAAGTACCCAACAATGTCACCTCTGAAGGAGGTTGTGGACAATATTCAGTCTCAGGT

TGCAAAAATTGAGGATGATCTCAAGGTATTGTAGCTTAAACCTTTTGTTTTATTGTAAAA
AAAAAGGAAGCTTCACCTTTAAGCAGAAAGATTAGCTGCATGAGACCGATGGTATAAAA
TTTGCAATTCGAGTTTCTTACGATGATCAAATGAATTGCTTTGGTTCAAATGGTGGTGTT
AACGACTCTGATTGCACATTTTATTCAGGTTCGTGTTGCTGAATATAACAATATCCGTGG
TCAACTCAATGCCATTAACCGAAAGCAAAGTGGAAGGTAATTCTTTTCTTCTCATATTTA
TACTATAAGAGCACACTAGAAACTGTGGGCGGTTTAGCAACAACAAATTTTGAAGTTTG
TTTTCTCATCTATCTGATTTTTGCTTGAAGCATGATTTACCACGTGAACGTTTTAGAATAA
TACAAAGTTATTTTCCAGAATATTGCTGTTGGTCTTTATCGATATCTCAGCTTTGTTTAGT
ATCTTTGTGGCATTGTGGCTGATCGTCCTCCTTTTTGTCTCAGCTTAGCTGTTCGTGAC
CTCTCAAACTTGGTTAAGCCAGAAGATATTGTCGAGTCCGAACATCTCGTAACTCTCCT
TGCAGTTGTTCCGAAGTATTCCCAAAAAGACTGGCTAGCATGTTATGAGACTTTGACC
GATTATGTGGTAAATTTGTTGACTTGCTAGGTTTATTGAATAGACCAGTGGTAACACTAC
TGGTTTGACGTACCGTGATTTTAATCAATTTATCCTAACTTGTTTCAGGTTCCTAGGTCC
TCGAAGAAATTGTTTGAGGATAATGAGTATGCCCTTTACACCGTCACTCTCTTTACTCG
TGTCGCAGATAATTTCAGGATTGCTGCTCGTGAGAAAGGATTCCAAGTGAGTATTCTGT
TCAAGTTCCTGATATTACCTCTAGAGTTACGTAGAAGTTAAAAATGATTACATGCTAGTA
GGAGTGAAATTTCCTACGAACTGATTGTATTCATGGTGCAAGTTCAGAAATTTGGTTTA
GATTCAAAGATTTGTTCATCATATATTGTACACCATCCTCTTCTAGGTCCGTGATTTTGAA
CAAAGTGTTGAAGCACAAGAGACTCGTAAACAAGAGCTAGCAAAGTTGGTTCAGGATC
AGGAAAGTTTGAGAAGCTCTCTTTTGCAGTGGTGCTACACCAGTTATGGAGAGGTAGG
TATCTACACATTGCTCTGAATAGATATTCTCTTGTAATACAATACCTGAATCTGTTTTGAT
CTTCGGTCTACATCTGTAGGTTTTCAGCTCCTGGATGCATTTCTGTGCTGTGCGTACAT
TCGCTGAGAGCATTATGAGATACGGTTTACCTCCGGCGTTCTTGGTAAATTAGGACTCC
AAGCTATGCTATTTTAGAGAATTCCTCTACCCTACTATCTCCCTTACCAAATTACTTTCTC
TTGTCTTTCCAGGCATGTGTCTTATCTCCGGCTGTGAAAAGTGAAAAGAAAGTACGCT
CCATTCTTGAACGCTTGTGTGATTCTACCAACAGGTATGTTAAAACTCTCTACCTATCTA
TCGCTCTAGGTGTAGGATACATGGAAGCTGTTTAACATCAACCTTCATATTGATCTGGC
GAAGAAAAATGTACTGATAGTTATGACCTTAATAACGAAAGAAATTGCAGAAGTTTGAG
GAGAAAGTCAGGAACCAAGTAAAACCAAACTTGTATTAGCATGCAATGCGTTCTTGAG
GCTAAATCTATTAATCAGAACTAAGTCGCTTTAGTTAGATTCATCTATTGATGTAGTGTAG
TTCGATGAGATTTCAAATTGAGCGTTTTGGGTCTCATTGTATGAAAACAATGCAGTTTAT
ACTGGAAAAGCGAGGAGGATGCAGGAGCCATGGCTGGTTTAGCTGGTGACTCAGAG
ACACATCCTTATGTCTCCTTCACTATCAACCTTGCTTAAAAATATGATGAGAGATGCTTT
TGATGCCACTTCTCCTCTGGTCTTCTCATCTGTTATATTTGTTTGTGGTCTATAGATTTCA
CATTTATTTTTCGTAACATATTTTGATTTTCATAAATAAGGTGGAACTCAAGAGAGATGTT
GCTGTAATTTTATTTGGCCGGAGTCTTTTAGATTCCGGCGAGTTTCAGACACTTGTGGA
AGACAGAAGGGTTATACAGTTGTTAAAGCCTTTTTGTCATTTTGTGACATGGTTGATTTA
TTTATATCATCACTCTGTTTCGTTTTTGTCTG

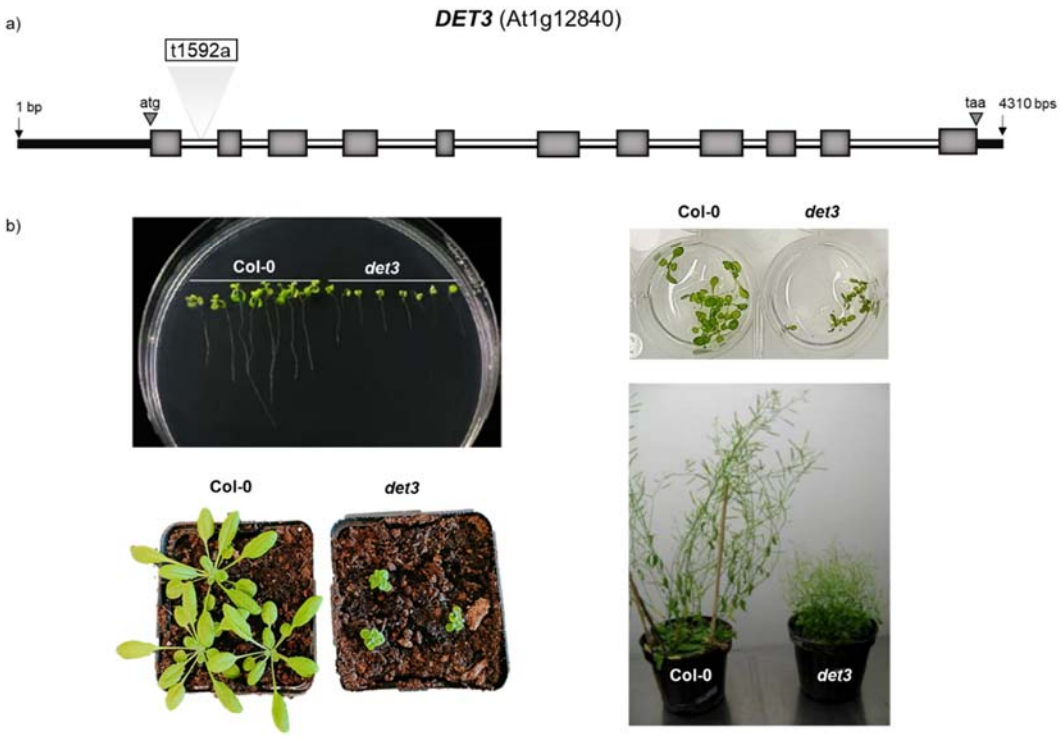

Supplementary Figure S1. Phenotype of *det3* mutant plant. a) Schematic representation of the genomic *DET3* sequence (At1g12840) showing the exons and introns as grey boxes and white lines, respectively. The specific location of the point mutation t1592a in the *det3* mutant is also indicated. b) Phenotype of wild type and *det3* plants in (up, *left*) 7-days old vertically grown seedlings, (up, *right*) 10-days old seedlings, (bottom, *left*) 4-weeks old and (bottom, *right*) mature plants.

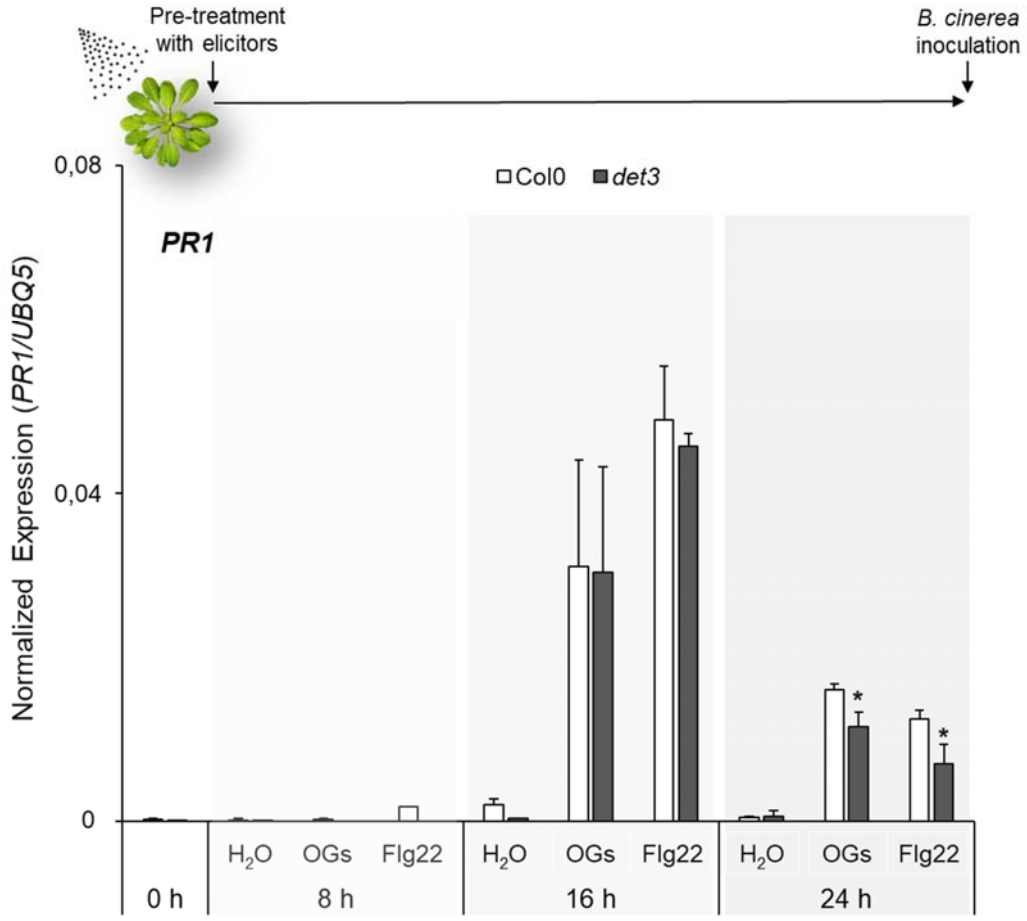

Supplementary Figure S2. Time-course analysis of *PR1* expression in adult leaves of plants sprayed with elicitors. The late defense gene *PR1* is induced at a lesser extent in *det3* mutant plant at 24h from elicitation. Adult plants were sprayed with water, OGs, and Flg22 and the leaves were collected at 0-, 8-, 16- and 24-h post-elicitation. The histogram shows *PR1* expression in the sprayed leaves from the wild type (WT; white bars) and *det3* mutant plants (dark-grey bars). The total RNA was extracted at the indicated times. *PR1* expression was evaluated by qRT-PCR using *UBQ5* as reference gene. Data represent the mean ± SD from three independent experiments. Asterisks indicate statistically significant differences between wild-type and the mutant by Student's t-test (*$p < 0.05$).

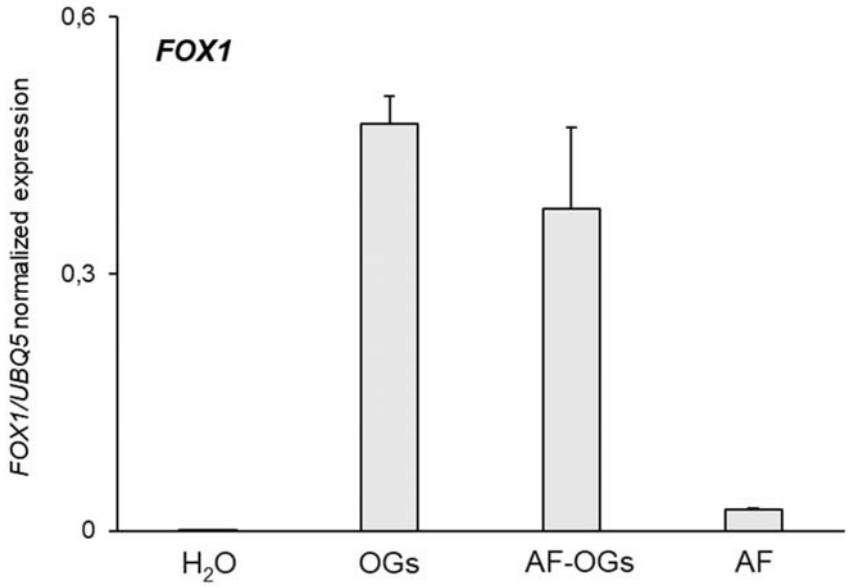

Supplementary Figure S3. Evaluation of elicitor activity of fluorescently labelled OGs. Arabidopsis wild-type seedlings were treated for 1 hour with water (H_2O), AlexaFluor labelled OGs (AF-OGs), OGs and AlexaFluor alone (AF). Expression of the defense marker gene *FOX1* was analyzed by qRT-PCR analysis, using the expression level of *UBQ5* as reference. Bars represent mean ± SD (n = 3).

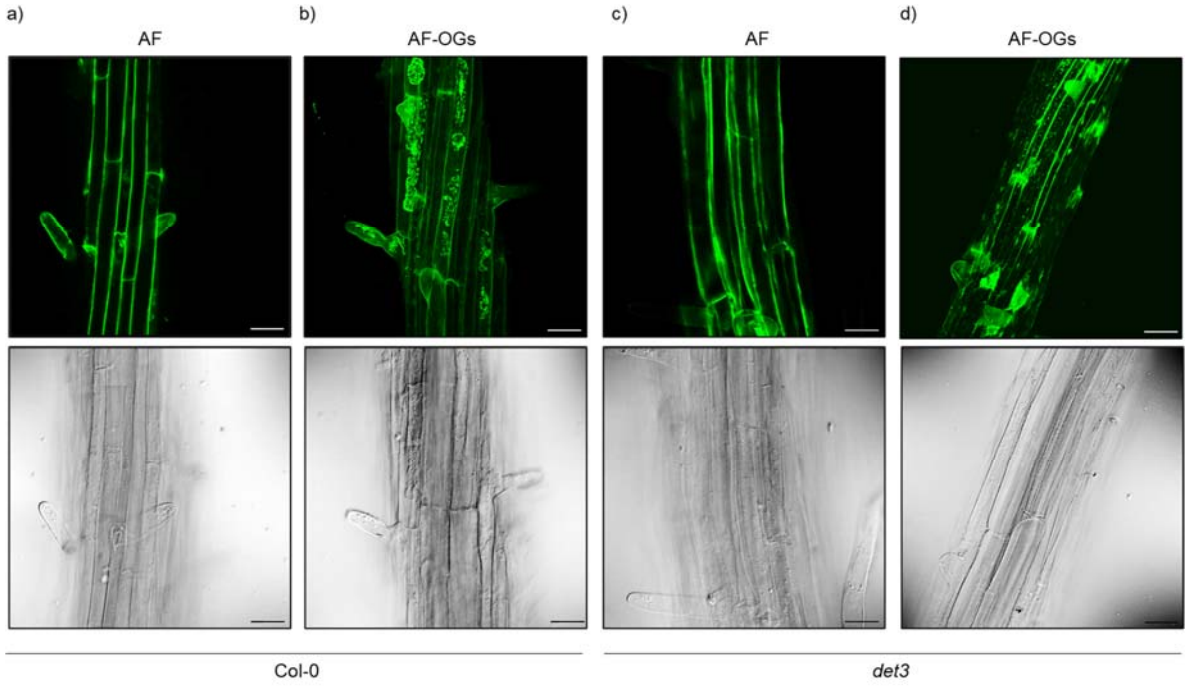

Supplementary Figure S4. Confocal microscopy analysis of wild type and *det3* roots upon treatment with AF-OGs. Confocal microscope analysis of roots from seven days old Col0 (a-b) and *det3* (c-d) seedlings after 30 minutes of treatment with (a, c) Alexa Fluor 488 alone (AF) and with (b, d) Alexa Fluor 488-labelled OGs (AF-OGs). For each treated plant, the corresponding bright field image is reported. Bars = 20 μm.

Supplementary Table S1. Primers used in this work.

GENE	ATG CODE	FORWARD PRIMER (5'->3')	REVERSE PRIMER (5'->3')
UBQ5	AT3G62250	GTTAAGCTCGCTGTTCTTCAGT	TCAAGCTTCAACTCCTTCTTTC
FOX1	AT1G26380	AGGTTCTCGAACCCTAACAACA	GCACAGACGACACGTAAGAAAG
CYP81F2	AT5G57220	GTGAAAGCACTAGGCGAAGC	ATCCGTTCCAGCTAGCATCA
PAD3	AT3G26830	CCGGTGAATCTTGAGAGAGCC	GATCAGCTCGGTCATTCCCC
PGIP1	AT5G06860	TCTTGAACTTAGCAGGAAC	GAGAGCTGGTTATGTGATAG